



# Polyunsaturated fatty acid metabolism in three fish species with different trophic level

A. Galindo<sup>a</sup>, D. Garrido<sup>a</sup>, Ó. Monroig<sup>b</sup>, J.A. Pérez<sup>a</sup>, M.B. Betancor<sup>c</sup>, N.G. Acosta<sup>a</sup>, N. Kabeya<sup>d</sup>, M.A. Marrero<sup>a</sup>, A. Bolaños<sup>a</sup>, C. Rodríguez<sup>a,\*</sup>

<sup>a</sup> Departamento de Biología Animal, Edafología y Geología, Universidad de La Laguna, Santa Cruz de Tenerife, Spain

<sup>b</sup> Instituto de Acuicultura Torre de la Sal, Consejo Superior de Investigaciones Científicas (IATS-CSIC), 12595 Ribera de Cabanes, Castellón, Spain

<sup>c</sup> Faculty of Natural Sciences, Institute of Aquaculture, University of Stirling, Stirling FK9 4LA, Scotland, United Kingdom

<sup>d</sup> Department of Marine Biosciences, Tokyo University of Marine Science and Technology, 4-5-7 Konan, Minato-ku, Tokyo, Japan

## ARTICLE INFO

### Keywords:

*Chelon labrosus*  
Elov15  
LC-PUFA  
*Pegusa lascaris*  
*Sarpa salpa*

## ABSTRACT

Reducing the dependency of fishfeed for marine ingredients and species diversification are both considered crucial factors for the sustainable development of aquaculture. The substitution of fish oil (FO) by vegetable oils (VO) in aquafeeds is an economically feasible solution. However, such substitution may compromise the fish flesh content of essential n-3 long chain polyunsaturated fatty acids (n-3 LC-PUFA) and, therefore, its nutritional value for human consumption. Likewise, there is a wide range of strategies to select new target species for sector diversification, among which, the capacity to biosynthesize n-3 LC-PUFA from their C<sub>18</sub> precursors abundant in VO might be considered as a fair preliminary strategy. Therefore, the aim of the present study was to analyze the metabolic fate of [1-<sup>14</sup>C] labeled 18:2n-6, 18:3n-3, 20:5n-3 and 22:6n-3 in isolated hepatocytes and enterocytes from wild individuals of three fish species with different trophic level: the marine herbivorous salem ( *Sarpa salpa* ), the strict carnivorous sand sole ( *Pegusa lascaris* ) and the omnivorous thicklip grey mullet ( *Chelon labrosus* ). These species were selected for their phylogenetic proximity to consolidated farmed species such as gilthead seabream ( *Sparus aurata* ), senegalese sole ( *Solea senegalensis* ), and golden grey mullet ( *Liza aurata* ), respectively. The study also assessed the molecular cloning, functional characterization and tissue distribution of the fatty acyl elongase (Elov1) gene, *elov15*, involved in the biosynthetic metabolism of n-3 LC-PUFA. The three species were able to biosynthesize docosahexaenoic acid (22:6n-3). *S. salpa* seems to have similar biosynthetic capacity than *S. aurata*, with a fatty acyl desaturase 2 (Fads2), with Δ6, Δ8 and Δ5 activities. *P. lascaris* showed a wider Fads2 activity repertory than *S. senegalensis*, including Δ4 and residual Δ6/Δ5 activities. In *C. labrosus*, both Δ8 and Δ5 activities but not the Δ6 described for *L. aurata* were detected in the incubated cells. Elongation from C<sub>18</sub> and C<sub>20</sub> precursors to C<sub>20</sub> and C<sub>22</sub> products occurred in hepatocytes and enterocytes as well as in the functional characterization of Elov15 by heterologous expression in yeast. Elov15 showed a species specific expression pattern, with the highest rates observed in the liver, gut and brain in *S. salpa* and *P. lascaris*, and in the brain for *C. labrosus*. In summary, the LC-PUFA biosynthesis capacity from *S. salpa*, *P. lascaris* and *C. labrosus* greatly resembled that of their phylogenetic closer species. The three studied species could be further explored as candidates for the aquaculture diversification from their potential ability to biosynthesize LC-PUFA.

## 1. Introduction

The annual *per capita* consumption of fish has risen up to 20.2 Kg in

2015, partly due to its contribution to the population needs for high-quality proteins, lipids and micronutrients (FAO, 2018). Lipids, and their main components, fatty acids (FA), are along with proteins, the

**Abbreviations:** ARA, arachidonic acid; BHT, butylated hydroxyl toluene; DHA, docosahexaenoic acid; dpm, desintegrations per minute; *ef1α*, elongation factor-1α; Elov15, fatty acyl elongase 5; EPA, eicosapentaenoic acid; FA, fatty acid; Fads2, fatty acyl desaturase 2; FAF-BSA, fatty acid free bovine serum albumin; FAME, fatty acid methyl esters; FID, flame ionization detector; FO, fish oil; HBSS, Hanks balanced salt solution; LC-PUFA, long chain polyunsaturated fatty acid; NTC, negative controls; ORF, open reading fragment; PCR, polymerase chain reaction; PUFA, polyunsaturated fatty acid; qPCR, quantification real-time PCR; RACE, rapid amplification of cDNA ends; TL, total lipid; VO, vegetable oils.

\* Corresponding author.

E-mail address: [covarodr@ull.edu.es](mailto:covarodr@ull.edu.es) (C. Rodríguez).

<https://doi.org/10.1016/j.aquaculture.2020.735761>

Received 8 May 2020; Received in revised form 29 June 2020; Accepted 23 July 2020

Available online 30 July 2020

0044-8486/ © 2020 Elsevier B.V. All rights reserved.

largest organic components of fish. C<sub>18</sub> polyunsaturated fatty acids (PUFA) such as 18:2n-6 and 18:3n-3, are considered essential nutrients for vertebrates because they cannot be synthesized *de novo*. Additionally, they are metabolic precursors of the physiologically important long-chain (C<sub>20–24</sub>) PUFA (LC-PUFA) including arachidonic (20:4n-6, ARA), eicosapentaenoic (20:5n-3, EPA), and docosahexaenoic (22:6n-3, DHA) acids (Tocher, 2015). LC-PUFA are involved in key roles including cell membrane structure, transcription, regulation and cellular signalling (Lee et al., 2016; Tocher, 2015; Zárate et al., 2017). Particularly, the n-3 LC-PUFA 20:5n-3 and 22:6n-3 have been seen to prevent several human inflammatory and neurodegenerative illnesses (Lee et al., 2016; Zárate et al., 2017).

Fish, including farmed species, are the primary source of n-3 LC-PUFA for humans (Bell and Tocher, 2009). However, the fluctuating availability of marine ingredients used in aquafeed formulation, namely fish oil (FO) and fishmeal, their sustained price increase, the increment of global aquaculture production and the necessity to search for more sustainable alternatives to feed carnivorous species have resulted in a pressing need for their partial replacement by ingredients of terrestrial origin such as vegetable oils (VO). This practice reduces the n-3 LC-PUFA content in fish muscle (Pérez et al., 2014; Tocher, 2015) and therefore, its nutritional value to consumers. Recently, the use of oils from transgenic plants and the inclusion of micro and macroalgae-origin products rich in n-3 LC-PUFA have been proposed as possible novel alternatives to marine sources (Ruyter et al., 2019; Sprague et al., 2016; Tocher et al., 2019). Moreover, farming of fish species with high capacity to biosynthesize LC-PUFA from their C<sub>18</sub> precursors abundant in VO may also be considered as a valuable sustainable strategy for the aquaculture industry (Garrido et al., 2019). Therefore, it is essential to understand the LC-PUFA metabolism of potential candidate species for the diversification of aquaculture in order to select fish with high capacity to utilize dietary VO while maintaining proper growth and development, as well as its nutritional quality in terms of n-3 LC-PUFA content.

Liver is the main organ involved in lipid metabolism while gut have an important role in both uptake and LC-PUFA biosynthesis. In this sense, the incorporation and bioconversion of radiolabeled FA in enterocytes and hepatocytes from fish species have been demonstrated as an adequate tool to elucidate their LC-PUFA biosynthesis capabilities (Díaz-López et al., 2010; Garrido et al., 2020; Morais et al., 2015; Mourente and Tocher, 1993a, 1993b, 1994; Rodríguez et al., 2002; Tocher and Ghioni, 1999).

LC-PUFA biosynthesis in vertebrates including fish, is mediated by two types of enzymes (Monroig et al., 2018). On the one hand, the fatty acyl elongase (Elovl) proteins catalyze the condensation reaction of the fatty acid elongation pathway resulting in the extension of the fatty acyl chain in two carbons. Thus, enzymes such as Elovl5, Elovl2 and Elovl4 are being extensively studied in fish (Castro et al., 2016; Garlito et al., 2019; Monroig et al., 2018). On the other hand, fatty acyl desaturases (Fads) enzymes enter a double bond to PUFA substrates in between an existing one and the carbon of the carboxylic group. The Greek letter ( $\Delta$ ) is used to denote the position of the double bond created by Fads in the hydrocarbon chain. Unlike mammalian FADS2 that typically have  $\Delta 6/\Delta 8$  activity (Castro et al., 2016), teleost Fads2 show high interspecific variability in their desaturase capacity. Thus, along with the  $\Delta 6/\Delta 8$  activity (Monroig et al., 2011a), Fads2 with  $\Delta 4$  and  $\Delta 5$ , as well as bifunctional  $\Delta 6/\Delta 5$  desaturases have been reported (Castro et al., 2016; Garrido et al., 2020; Monroig et al., 2011a, 2018). The production of 20:4n-6 and 20:5n-3 from 18:2n-6 or 18:3n-3, respectively, may be obtained by a  $\Delta 6$  desaturation activity towards C<sub>18</sub> substrates followed by an elongation step and a final  $\Delta 5$  desaturation (Fig. 1). Alternatively, a  $\Delta 8$  desaturation over C<sub>20</sub> intermediates may be also involved in the production of 20:4n-6 and 20:5n-3 from C<sub>18</sub> precursors (Monroig et al., 2011a). The biosynthesis of 22:6n-3 from 20:5n-3 can be mediated via the Sprecher pathway (Sprecher, 2000), which requires two consecutive elongation steps, a  $\Delta 6$  desaturation, and a final

peroxisomal  $\beta$ -oxidation or through an alternative and more direct route with the action of a  $\Delta 4$  desaturase (Li et al., 2010; Oboh et al., 2017) (Fig. 1).

The biosynthetic ability of each species to biosynthesize LC-PUFA was believed until very recently to depend on the species' habitat (freshwater vs marine), with marine species having limited capacity to convert C<sub>18</sub> PUFA to LC-PUFA, and freshwater/diadromous fish having retained the ability to elongate and desaturate C<sub>18</sub> precursors (Garrido et al., 2019; Monroig et al., 2018). Such generalization was questioned when the marine herbivore, *Siganus canaliculatus*, was reported to have a  $\Delta 4$  Fads2 and a bifunctional  $\Delta 5/\Delta 6$  Fads2 (Li et al., 2010). Further studies demonstrated the presence of  $\Delta 4$  Fads2 in teleost species from a variety of habitats and trophic levels (Fonseca-Madrigras et al., 2014; Garrido et al., 2019; Kuah et al., 2015; Morais et al., 2012, 2015; Oboh et al., 2017). Thus, other factors such as phylogeny have been recently pointed out to influence the LC-PUFA biosynthetic capacity of teleosts (Castro et al., 2016; Garrido et al., 2019; Monroig et al., 2018). In teleosts, Elovl5 and Elovl2 share a common evolutionary origin (Monroig et al., 2016), and consequently, both of them have preference for C<sub>18</sub> and C<sub>20</sub> PUFA substrates although Elovl5 has also been reported to present some affinity towards C<sub>22</sub> PUFA (Monroig et al., 2012).

In order to explore the potentiality of a wider range of species for the diversification of finfish aquaculture, based on their n-3 LC-PUFA biosynthesis capabilities, three fish species with different trophic levels were selected in the present study: the salema *Sarpa salpa* (Linnaeus, 1758), a marine herbivorous of the Sparidae family with trophic affinity with *S. canaliculatus*; the sand sole *Pegusa lascaris* (Risso, 1810), a strict carnivorous member of the Soleidae family that is phylogenetically close to *Solea senegalensis*; and the thicklip grey mullet *Chelon labrosus* (Risso, 1827), a species from the Mugilidae family closely related to *Liza aurata* with high adaptability to different feeding habits. Molecular cloning, functional characterization and tissue distribution of  $\Delta 6$  and  $\Delta 8$  desaturase have been already described by our group in *S. salpa* and *C. labrosus*, as well as  $\Delta 4$  desaturase in *P. lascaris* (Garrido et al., 2019). However, their LC-PUFA metabolism capacities were not completely characterized. To this aim, isolated enterocytes and hepatocytes were incubated with different PUFA substrates, in order to compare their uptake affinities and the ability of Fads2 and Elovl to desaturate and elongate C<sub>18</sub> and C<sub>20</sub> radiolabeled FA precursors. Furthermore, the molecular cloning, functional characterization and tissue distribution of *elov5* elongases were also elucidated. The results of the present study are discussed within the context of fish nutrition and their applicability to the diversification of aquaculture with species able to efficiently utilize ingredients alternative to FO.

## 2. Material and methods

### 2.1. Experimental animals and sampling

All experimental procedures were approved by the Ethical Committee at the University of La Laguna and were in accordance with the EU Directive 2010/63 regarding the protection and humane use of animals for scientific purpose.

Wild specimens of *S. salpa* (87.4 ± 14.4 g; n = 5) and *C. labrosus* (12.5 ± 9.1 g; n = 6) were captured by professional artisanal fishermen in Tenerife (Spain), while *P. lascaris* (111.2 ± 25.5 g; n = 3) were captured off the coast of Huelva (Spain). Fish were subsequently transported to the laboratory for sacrifice and subsequent sampling. Samples of muscle, liver, heart, foregut, brain and gill were collected for molecular cloning, functional characterization and tissue distribution. Tissues were kept in RNAlater (Qiagen Iberia SL, Madrid, Spain) the first 24 h at 4 °C and then stored at -20 °C until analysis. In addition, the remaining foregut and liver were rapidly taken for the isolation of enterocytes and hepatocytes, respectively. The isolated cells were used for incubation and final extraction of the total lipid (TL) required to either assess the FA composition of control cells or to evaluate the

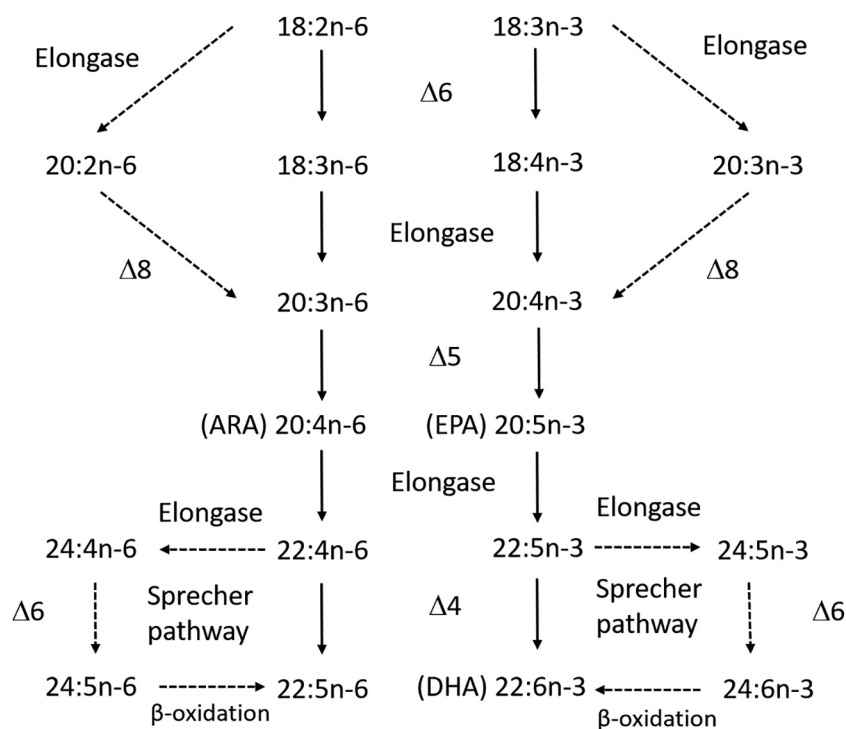


Fig. 1. Long-chain (C20–24) polyunsaturated fatty acids biosynthetic route from linoleic (n-6) and  $\alpha$ -linolenic acid (n-3).

incorporation of radioactivity into TL and the bioconversion rates of FA in the radiolabeled  $[1-^{14}\text{C}]$  incubated cells. Furthermore, muscle samples were also used for lipid and FA composition determination. The whole process was developed under an ice-cold environment to prevent sample degradation.

## 2.2. Isolation of enterocytes and hepatocytes and incubation with radiolabeled $[1-^{14}\text{C}]$ fatty acids

Enterocytes and hepatocytes were obtained as described by Rodríguez et al. (2002). Organs from two or more fish were pooled in the case of *P. lascaris* and *C. labrosus* due to the small size of the animals. Before the beginning of the experiments, the foregut was cleaned of food and feces and the liver perfused through the hepatic portal vein with a solution of marine Ringer containing 116 mM NaCl, 6 mM KCl, 1 mM  $\text{CaCl}_2$ , 1 mM  $\text{MgSO}_4$ , 10 mM  $\text{NaHCO}_3$ , 1 mM  $\text{NaH}_2\text{PO}_4$ , 10 mM  $\text{K}_2\text{SO}_4$  and 10 mM HEPES (pH 7.4). Tissues were minced in Hanks balanced salt solution (HBSS) with NaCl 1.75% (w/v) (HBSS/NaCl), 9.69 mM HEPES, 1.73 mM  $\text{NaHCO}_3$ , and collagenase (10 mg/mL) and incubated with HBSS/collagenase in agitation for 40 min at 20 °C. The resultant cell suspensions were filtered through a 100  $\mu\text{m}$  nylon mesh with HBSS including 1% (w/v) fatty acid free bovine serum albumin (FAF-BSA). Cells were collected by centrifugation (Beckman Coulter Allegra 25R, Indianapolis, USA) at 716g for 10 min, washed with HBSS and re-centrifuged for 7 min. The isolated cells were then re-suspended in cold M199 medium with NaCl and a sample was taken to assess the viability of cells (over 90% in all cases) by using the trypan blue exclusion test.

Immediately after isolation, 6 mL of each cell preparation were incubated in sterile plastic flasks for 3 h with 40  $\mu\text{L}$  (0.20  $\mu\text{Ci}$ ) of radiolabeled  $[1-^{14}\text{C}]$  PUFA: 18:2n-6, 18:3n-3, 20:5n-3 or 22:6n-3, with specific activities of 124.3, 114.8, 122.1 and 122.1 dpm  $\text{pmol}^{-1}$ , respectively. A control incubation of 2 mL of each cell type suspension without the addition of radiolabeled FA was also performed under the same experimental conditions for the determination of FA profiles. Samples were stored at  $-80$  °C until analysis.

## 2.3. Lipid extraction and protein determination

The TL content of isolated cells (enterocytes and hepatocytes) was extracted after incubation with small modifications of the Folch method (Folch et al., 1957) as described by Christie and Han (2010). Briefly, either incubated control or radioactive cell preparations, were transferred into test tubes, centrifuged at 716g for 5 min and the resultant pellets re-suspended in 4 mL of HBSS and re-centrifuged. Pellets were dissolved in 2 mL of 0.88% KCl (w/v), and 8 mL of chloroform/methanol (2:1, v/v) containing 0.01% (w/v) butylated hydroxytoluene (BHT) as antioxidant. After vigorous shaking, samples were re-centrifuged at 716g for 5 min, the organic solvent collected, filtered, and evaporated under a stream of nitrogen. The TL content was determined gravimetrically, re-suspended in chloroform/methanol (2:1, v/v) with 0.01% (w/v) BHT and stored at  $-20$  °C under an atmosphere of nitrogen until further analysis. For the lipid extraction of muscle samples, the same procedure as described above was performed, but tissue was previously homogenized in chloroform/methanol (2:1, v/v) using a Virtis rotor homogenizer (Virtishear, Virtis, Gardiner, New York).

Total protein content of incubated enterocytes and hepatocytes was determined in 100  $\mu\text{L}$ -aliquots of cell suspensions, according to Lowry et al. (1951) using FAF-BSA as standard.

## 2.4. FA composition of non-radioactive samples

In order to assess the baseline FA composition of liver and gut epithelial cells from the three species, a smaller fraction (2 mL) of isolated enterocytes and hepatocytes suspensions that had been also incubated without  $[1-^{14}\text{C}]$  PUFA, were finally analyzed. Up to 1 mg of TL extracted from these control cell suspensions and from muscle samples were subjected to acid-catalyzed transmethylation to obtain fatty acid methyl esters (FAME). Resultant FAME were purified by thin-layer chromatography (Macherey-Nagel, Düren, Germany), separated and quantified using a TRACE-GC Ultra gas chromatograph (Thermo Scientific, Milan, Italy) equipped with an on-column injection, a flame ionization detector (FID) and a fused silica capillary column Supelcowax® 10 (30 m  $\times$  0.32 mm ID, df 0.25  $\mu\text{m}$ ) (Supelco Inc.,

Bellefonte, USA). Helium was used as the carrier gas at 1.5 mL/min constant flow, and temperature programming was from 50 to 150 °C at a rate of 40 °C/min, then from 150 °C to 200 °C at 2 °C/min, to 214 °C at 1 °C/min and, finally, to 230 °C at 40 °C/min, which was maintained for 3 min. Individual FAME were identified by reference to authentic standards and further confirmation of FAME identity was carried out by GC-MS (DSQ II, Thermo Scientific) when necessary. The results are expressed as percentage of total FA.

Muscle FA composition of the three studied species is shown in the supplementary data table.

## 2.5. Metabolic fate of [ $^{14}\text{C}$ ] PUFA. Incorporation of radioactivity into TL and bioconversion of radiolabeled FA

A 100 µg aliquot of TL from cells incubated with each radiolabeled FA (18:2n-6, 18:3n-3, 20:5n-3 or 22:6n-3) was used to determine the radioactivity incorporated by means of a liquid scintillation β-counter (TRI-CARB 4810TR, Perkin Elmer, Singapore). Results obtained in dpm were related to the specific activity of each fatty acid and to the cells TL and protein contents, and expressed as pmol mg prot<sup>-1</sup> h<sup>-1</sup>.

Desaturation-elongation capacities of isolated enterocytes and hepatocytes from the three fish species incubated with [ $^{14}\text{C}$ ] PUFA (18:2n-6, 18:3n-3 and 20:5n-3) were determined using aliquots of up to 1 mg of the TL extract. Samples were subjected to acid-catalyzed transmethylation and the resultant FAME were then purified by argentation thin layer chromatography (AgNO<sub>3</sub>-TLC) using TLC plates previously impregnated with 2 g silver nitrate in 20 mL acetonitrile and activated at 110 °C for 30 min. A known standard composed by a mixture of radiolabeled FA was also developed in the same plates for the identification of each band. TLC plates were fully developed in toluene/acetonitrile (95:5, v/v) to separate the bands of [ $^{14}\text{C}$ ] FA (Wilson and Sargent, 1992). Then, they were placed in closed exposure cassettes in contact with a radioactive-sensitive phosphor screen (Exposure Cassette-K, BioRad, Madrid, Spain) for 2 weeks. Screens were scanned with an image acquisition system (Molecular Imager Fx, BioRad), and bands were identified and quantified in percentage of area using Quantity One 4.5.2. (BioRad) image software.

## 2.6. Molecular cloning of *elovl5* cDNAs

Total RNA was extracted from each tissue (muscle, heart, liver, gut, brain and gill) and species using TRI Reagent (Sigma-Aldrich, Dorset, UK) following the manufacturer's instructions and using a bead tissue disruptor (Bio Spec, Bartlesville, Oklahoma, USA). Next, cDNA was synthesized from 2 µg of total RNA (mixture from brain and liver; 1:1) for each species using a High Capacity cDNA Reverse Transcription Kit (Applied Biosystems, California, USA) for molecular cloning. Subsequently, the first fragment of *elovl5* genes for each species were obtained by polymerase chain reaction (PCR) using the cDNA as template together with degenerated primers (Table 1) and GoTaq® Green Master Mix (Promega, Southampton, UK). The degenerated primers for *elovl5* were designed on conserved regions from sequences obtained from NCBI blastn tool (<http://www.ncbi.nlm.nih.gov/>) of several teleosts including *S. canaliculatus* (GU597350.1), *Epinephelus coioides* (KF006241.1), *Rachycentron canadum* (FJ440239.1), *S. senegalensis* (JN793448.1), *Chirostoma estor* (KJ417837.1), *S. aurata* (AY660879.1) and *Salmo salar* (NM\_001123567.2). The alignment of *elovl5* sequences was carried out with BioEdit v7.0.9 (Tom Hall, Department of Microbiology, North Carolina State University, North Carolina, USA). The amplification of the first fragments by PCR were performed by an initial denaturing step at 95 °C for 2 min, followed by the PCR conditions shown in Table 2 for each primer set, followed by a final extension at 72 °C for 5 min. The amplified PCR fragments were purified on agarose gels using Illustra™ GFX™ PCR DNA and Gel Band Purification kit (GE Healthcare Life Sciences, Buckinghamshire, UK) and cloned into pGEM-T Easy vector (Promega) and sequenced (GATC Biotech, Konstanz,

Germany). Then, the obtained sequences were used for designing specific primers that allowed obtaining the 5' and 3' regions by Rapid Amplification of cDNA Ends (RACE). The cDNA for RACE was prepared by FirstChoice® RLM-RACE kit (Ambion, Applied Biosystems, Warrington, UK) following manufacturer's recommendations. All RACE PCR conditions and primers used are also reported in Tables 1 and 2. After the nested PCR using the first PCR product as a template, we successfully amplified each cDNA ends fragment. All RACE fragments were sequenced as described above and assembled with the corresponding first-fragments to obtain putative full-length cDNA.

## 2.7. Sequence and phylogenetic analyses

The deduced amino acid (aa) sequences of putative *Elov15* proteins isolated from *S. salpa*, *P. lascaris* and *C. labrosus* with a variety of functionally characterized *Elov12*, *Elov14* and *Elov15* from vertebrates (human and fish) retrieved from NCBI were aligned using MAFFT (<https://mafft.cbrc.jp/alignment/software/>) Ver. 7.388 with the *E-INS-i* strategy (Katoh et al., 2019). All columns containing gaps in the obtained alignment were removed by trimAl (Capella-Gutiérrez et al., 2009). The cleaned alignment was subjected to a maximum likelihood phylogenetic analysis using RAxML with 1000 rapid bootstrap replicates. The best-fit evolutionary model was selected to LG + G + I for both genes by ModelTest-NG (Darriba et al., 2020). The resultant RAxML tree was visualized using Interactive Tree of Life v3 (Letunic and Bork, 2016).

## 2.8. Functional characterization

The open reading frames (ORF) of *elovl5* were amplified from *S. salpa*, *P. lascaris* and *C. labrosus* from liver cDNA by a nested PCR approach. All primers and PCR conditions are described in Tables 1 and 2. First-round of PCR used primer pairs designed for each species in the 5' and 3' untranslated regions (UTR) for forward and reverse primers, respectively. Second round of PCR was run using the first-round PCR products as templates and primers containing restriction sites (underlined in Table 1) for subsequent ligation into the yeast expression vector pYES2 (Thermo Fisher Scientific, Hemel Hempstead, UK). In the case of *P. lascaris*, both first and second round PCR were performed with the high fidelity *Pfu* DNA polymerase (Promega), whereas for *S. salpa* and *C. labrosus elovl5* the *PfuUltra II Fusion HS DNA Polymerase* (Agilent, Santa Clara, California, USA) was used. Subsequently, the PCR products were purified, digested with the corresponding restriction enzymes (New England BioLabs, Hitchin, UK) and ligated into a similarly restricted pYES2. The plasmids containing pYES2-*elovl5* from each species were purified (GenElute™ Plasmid Miniprep Kit, Sigma) and sequenced before being transformed into yeast *Saccharomyces cerevisiae* competent cells InvSc1 (Thermo Fisher Scientific). Transformation and selection of yeast culture were performed as described by Garrido et al. (2019). One single yeast colony transformed with pYES2-*elovl5* for each species was used for functional assays. The transgenic yeasts were grown in the presence of one of the potential FA substrates for elongases, namely 18:2n-6, 18:3n-3, 18:3n-6, 18:4n-3, 20:4n-6, 20:5n-3, 22:4n-6 and 22:5n-3. The FA substrates were added to the yeast cultures at final concentrations of 0.5 mM (C<sub>18</sub>), 0.75 mM (C<sub>20</sub>) and 1.0 mM (C<sub>22</sub>) as uptake efficiency decreases with increasing chain length (Kabeya et al., 2018). In addition, yeasts transformed with empty pYES2 were also grown in the presence of each substrate as control treatments. After 2 days of culture at 30 °C, yeasts were harvested, washed, and TL extracted by homogenization in chloroform/methanol (2:1, v/v) containing 0.01% (w/v) BHT as antioxidant.

## 2.9. Fatty acid analysis of yeast

FAME were determined from the TL extracted from yeast according to Hastings et al. (2001). FAME were separated and quantified using a

**Table 1**

Sequences of primer pairs used in the cloning of *Sarpa salpa*, *Pegusa lascaris*, and *Chelon labrosus* fatty acyl elongase (*elovl5*) open reading frame (ORF) and for quantitative real-time PCR (qPCR) analysis of gene expression in tissues.

Aim	Species	Transcript	Primers	Primers sequence
First fragment	<i>S. salpa</i>	<i>elovl5</i>	FFElov15F1	5'- TACCCDCCAACCTTGGCACT -3'
			FFElov15R1	5'- TCAATCCACCCTCAGCTTCTTG -3'
	<i>P. lascaris</i>		FFElov15F1	5'- TACCCDCCAACCTTGGCACT -3'
RACE PCR	<i>S. salpa</i>	<i>elovl5</i>	FFElov15R2	5'- TCAATCCACCCTYAGYTTCTTG -3'
			FFElov15F1	5'- TACCCDCCAACCTTGGCACT -3'
			FFElov15R2	5'- TCAATCCACCCTYAGYTTCTTG -3'
	<i>P. lascaris</i>	<i>elovl5</i>	3'SSElov15F1	5'- CCGTACCTTTGGTGAAGAAGT -3'
			3'SSElov15F2	5'- CAGTTCAGCTGATCCAGTTCT -3'
			5'SSElov15R1	5'- TTCATGTACTTGGGCCCATC -3'
ORF cloning	<i>S. salpa</i>	<i>elovl5</i>	5'SSElov15R2	5'- GGTGGGTAGTTGTCGAGCAG -3'
			3'PLElov15F1	5'- CCCATGCGATGGCTATACTT -3'
			3'PLElov15F2	5'- ACGTACAAGAAGCGCAGTGT -3'
	<i>P. lascaris</i>	<i>elovl5</i>	5'PLElov15R1	5'- GTAGAAGTTGTAGCCCCGTG -3'
			5'PLElov15R2	5'- TGTAGAGCACCAGAAGGCCT -3'
			3'CLElov15F1	5'- ACATGTTCACTCACCATCCT -3'
qPCR	<i>S. salpa</i>	<i>elovl5</i>	3'CLElov15F2	5'- TCAGACTTACAAAAGCGCAGC -3'
			5'CLElov15R1	5'- CTCTCTCGCGCTGTGAGT -3'
			5'CLElov15R2	5'- TTGTAGCCACCATGCCACAC -3'
	<i>P. lascaris</i>	<i>elovl5</i>	SSElov15UF	5'-CTCTCCCTCTCGAAAAGGTG -3'
			SSElov15UR	5'-GAGAAATGGGGTGACGGTTTCTCAAATG-3'
			SSElov15VF	5'-CCC <u>GGATCC</u> AAAATGGAGACCTTC-3'
qPCR	<i>P. lascaris</i>	<i>elovl5</i>	SSElov15VR	5'-CCG <u>CTCGAGT</u> CAATCCACTCTCAG-3'
			PLElov15UF	5'-GTGTGTGTAATCGCTGATCTTCATGG-3'
			PLElov15UR	5'-GATGTTGGGTGATACTTCTCAAAGG-3'
	<i>C. labrosus</i>	<i>elovl5</i>	PLElov15VF	5'-CCC <u>GGATCC</u> AAAATGGAGACCTTC-3'
			PLElov15VR	5'-CCG <u>CTCGAGT</u> CAATCCACCCTTAG-3'
			CLElov15UF	5'-GGCTGGGCGACTTGATGGTG-3'
qPCR	<i>S. salpa</i>	<i>elovl5</i>	CLElov15UR	5'-CCTCCTAGCAGCATTAGCTAACAC-3'
			CLElov15VF	5'-CCC <u>GGATCC</u> AAAATGGAGGCCTTC-3'
			CLElov15VR	5'- CCG <u>CTCGAGT</u> CAATCCACCCTC-3'
	<i>P. lascaris</i>	<i>elovl5</i>	SSElov15qF1	5'-ACAAGCACAGTGCGTCTCTAA-3'
			SSElov15qR1	5'-ACGCACTACAGTGAGAATGGG-3'
			PLElov15qF1	5'-GCTGACAAAACCTGGAGAGC-3'
	<i>C. labrosus</i>	<i>elovl5</i>	PLElov15qR1	5'-CCTCTGGATGTCTTTTGA-3'
			CLElov15qF1	5'-AGAACGGCTCCTCCCTATCA-3'
			CLElov15qR1	5'-CAGCATTAGCTAACACGCTACA-3'
	<i>S. salpa</i>	$\beta$ -actin	$\beta$ -actinqF1	5'-CAGGGAGAAGATGACCCAGA-3'
			$\beta$ -actinqR1	5'-ACAGTGCCCATCTATGAGGG-3'
			$\beta$ -actinqF1	5'-CAGGGAGAAGATGACCCAGA-3'
<i>P. lascaris</i>	$\beta$ -actin	$\beta$ -actinqR1	5'-ACAGTGCCCATCTATGAGGG-3'	
		$\beta$ -actinqF1	5'-CAGGGAGAAGATGACCCAGA-3'	
		$\beta$ -actinqR2	5'-CCCTCGTAGATGGGCACTGT-3'	
<i>C. labrosus</i>	$\beta$ -actin	$\beta$ -actinqF1	5'-CCCTCGTAGATGGGCACTGT-3'	
		$\beta$ -actinqR1	5'-ATGCACCACGAGTCTCTGAC-3'	
		$\beta$ -actinqR2	5'-GGGTGGTTCAGGATGATGAC-3'	
<i>S. salpa</i>	<i>efl1<math>\alpha</math></i>	<i>efl1</i> aqF1	5'-GTGGAGATGCACCACGATC-3'	
		<i>efl1</i> aqR1	5'-GGGTGGTTCAGGATGATGAC-3'	
		<i>efl1</i> aqF2	5'-GTGGAGATGCACCACGATC-3'	
<i>P. lascaris</i>	<i>efl1<math>\alpha</math></i>	<i>efl1</i> aqR1	5'-GGGTGGTTCAGGATGATGAC-3'	
		<i>efl1</i> aqF2	5'-GTCGAGATGCACCACGATC-3'	
		<i>efl1</i> aqR1	5'-GGGTGGTTCAGGATGATGAC-3'	
<i>C. labrosus</i>	<i>efl1<math>\alpha</math></i>	<i>efl1</i> aqF3	5'-GTCGAGATGCACCACGATC-3'	
		<i>efl1</i> aqR1	5'-GGGTGGTTCAGGATGATGAC-3'	
		<i>efl1</i> aqR1	5'-GGGTGGTTCAGGATGATGAC-3'	

Restriction sites *Bam*HI/*Xho*I for *S. salpa* (SSElov15VF/SSElov15VR), *P. lascaris* (PLElov15VF/PLElov15VR) and *C. labrosus* (CLElov15VF/CLElov15VR) are underlined in the corresponding primer sequences.

Fisons GC-8160 (Thermo Fisher Scientific) gas chromatograph equipped with a 60 m  $\times$  0.32 mm i.d.  $\times$  0.25  $\mu$ m ZB-wax column (Phenomenex, Macclesfield, UK) and FID. The elongation conversion efficiencies from exogenously added PUFA substrates were calculated by the proportion of substrate FA converted to elongated products as [product area/(product area + substrate area)]  $\times$  100.

## 2.10. Tissue expression of *elovl5*

Expression of the *elovl5* gene was determined by quantitative real-time PCR (qPCR) in muscle, heart, liver, gut, brain and gill, being the number of replicates  $n = 4$  in *S. salpa* and *P. lascaris*, and  $n = 3$  in *C. labrosus*. Elongation factor-1 $\alpha$  (*efl1 $\alpha$* ) and  $\beta$ -actin (*actb*) and 18S were tested as potential reference genes for normalization of *elovl5* expression, with *efl1 $\alpha$*  and *actb* being selected for that purpose since they were the most stable genes according to geNorm (M stability value = 0.165;

Vandesompele et al., 2002). Total RNA was extracted and 2  $\mu$ g of each sample were reverse transcribed into cDNA as described above. In the interest of assessing the efficiency of the primer pairs, serial dilutions of pooled cDNA were carried out for each species. All qPCR were performed by a Biometra TOptical Thermocycler (Analytik Jena, Jena, Germany) in 96-well plates in duplicates at total volume of 20  $\mu$ L containing 10  $\mu$ L of Luminaris Color HiGreen qPCR Master Mix (Thermo Fisher Scientific), 1  $\mu$ L of each primer (10  $\mu$ M), 2  $\mu$ L or 5  $\mu$ L of cDNA (1/20 dilutions) for reference and target genes, respectively, as well as 6 or 3  $\mu$ L of molecular biology grade water. Besides, negative controls (NTC, no template control), containing molecular biology grade water instead of cDNA, were also run in each plate. The primer sequences and qPCR conditions are detailed in Tables 1 and 2, respectively. The relative expression of *elovl5* among tissues in each species was calculated as arbitrary units after normalization dividing by the geometric mean of the expression level of the reference genes *efl1 $\alpha$*

**Table 2**Reaction conditions for cloning, functional characterization and gene expression of *elovl5* in *Sarpa salpa*, *Pegusa lascaris* and *Chelon labrosus*.

Aim	Species	Transcript	Forward primer	Reverse primer	Denaturing temperature (°C) (duration in s)	Annealing temperature (°C) (duration in s)	Extension temperature (°C) (duration in s)	Number of cycles	
First fragment	<i>S. salpa</i>	<i>elovl5</i>	FFElov15F1	FFElov15R1	95 (30)	56 (45)	72 (60)	35	
	<i>P. lascaris</i>		FFElov15F1	FFElov15R2	"	"	"	"	
	<i>C. labrosus</i>		FFElov15F1	FFElov15R2	"	"	"	"	
RACE PCR	<i>S. salpa</i>	<i>elovl5</i>	5' RACE Outer	5'SSElov15R1	95 (30)	57 (30)	72 (90)	35	
			5' RACE Inner	5'SSElov15R2	"	"	"	"	
			3'SSElov15F1	3' RACE Outer	"	"	"	"	
			3'SSElov15F2	3' RACE Inner	"	"	"	"	
			<i>P. lascaris</i>	5' RACE Outer	5'PLElov15R1	95 (30)	57 (30)	72 (90)	35
				5' RACE Inner	5'PLElov15R2	"	"	"	"
	<i>C. labrosus</i>	<i>elovl5</i>	3'PLElov15F1	3' RACE Outer	"	"	"	"	
			3'PLElov15F2	3' RACE Inner	"	"	"	"	
			5' RACE Outer	5'CLElov15R1	"	"	"	"	
			5' RACE Inner	5'CLElov15R2	"	"	"	"	
			3'CLElov15F1	3' RACE Outer	"	"	"	"	
			3'CLElov15F2	3' RACE Inner	"	59 (30)	"	"	
ORF cloning	<i>S. salpa</i>	<i>elovl5</i>	SSElov15UF	SSElov15UR	95 (20)	55 (20)	72 (105)	40	
			SSElov15VF	SSElov15VR	"	"	"	"	
	<i>P. lascaris</i>	<i>elovl5</i>	PLElov15UF	PLElov15UR	95 (20)	55 (20)	72 (105)	35	
			PLElov15VF	PLElov15VR	"	"	"	"	
	<i>C. labrosus</i>	<i>elovl5</i>	CLElov15UF	CLElov15UR	95 (20)	55 (20)	72 (105)	40	
			CLElov15VF	CLElov15VR	"	"	"	"	
qPCR	<i>S. salpa</i>	<i>elovl5</i>	SSElov15qF1	SSElov15qR1	95 (15)	58.5 (30)	72 (30)	35	
			PLElov15qF1	PLElov15qR1	"	"	"	"	
			CLElov15qF1	CLElov15qR1	"	"	"	"	
	<i>S. salpa</i>	$\beta$ -actin	$\beta$ -actinqF1	$\beta$ -actinqR1	"	"	"	"	
			<i>P. lascaris</i>	$\beta$ -actinqF1	$\beta$ -actinqR1	"	"	"	"
				<i>C. labrosus</i>	$\beta$ -actinqF1	$\beta$ -actinqR2	"	"	"
	<i>S. salpa</i>	<i>efl1a</i>	<i>efl1a</i> qF1		<i>efl1a</i> qR1	"	"	"	"
			<i>P. lascaris</i>	<i>efl1a</i> qF2	<i>efl1a</i> qR1	"	"	"	"
	<i>C. labrosus</i>	<i>efl1a</i> qF3		<i>efl1a</i> qR1	"	"	"	"	

and *actb*. One arbitrary unit is defined as the ratio between the expression level of *elovl5* and the lowest expression level for this gene. After each qPCR analysis, a melting curve with 1 °C increments during 6 s from 60 to 95 °C was performed, in order to check the presence of a single product in each reaction.

### 2.11. Statistical analysis

Results for TL, FA composition, incorporation of radioactivity into TL, and bioconversions of enterocytes and hepatocytes incubated with [1-<sup>14</sup>C] FA substrates are presented as mean  $\pm$  SD (n = 5 for *S. salpa*, except for [1-<sup>14</sup>C] 22:6n-3 where n = 4; n = 6 for *C. labrosus* and n = 3 for *P. lascaris*). Tissue expression is presented as log 10 mean normalized ratios  $\pm$  standard error (N). *P* values of less than 0.05 were considered significantly different for all statistical test applied. Normal distribution of the data and homogeneity of the variances were verified with the one-sample Shapiro-Wilk test and the Levene test, respectively (Zar, 1999).

Statistical differences in the incorporation of radioactivity into TL in enterocytes and hepatocytes incubated with [1-<sup>14</sup>C]FA substrates (18:2n-6, 18:3n-3, 20:5n-3 and 22:6n-3), the bioconversions of [1-<sup>14</sup>C] FA substrates in enterocytes and hepatocytes (18:2n-6, 18:3n-3 and 20:5n-3) as well as tissue expression were tested by one-way ANOVA followed by a Tukey HSD multiple comparison test (Zar, 1999) for each cell type and species. When homocedasticity was not achieved, data were transformed using logarithm or arcsine square root. If transformations did not succeed, Welch test was performed, followed by T3 Dunnett. Kruskal-Wallis non-parametric test was applied in the case of no normal distribution followed by pair-wise comparisons Mann-Whitney test with Bonferroni correction. When one group was missing, the remaining two groups were analyzed by t-student or Mann-Whitney tests for no normal data. All statistical analyses were performed using the IBM SPSS statistics 25.0 for Windows (SPSS Inc., New York, USA).

## 3. Results

### 3.1. Lipid content and fatty acid composition of control cells, and incorporation of radioactivity into total lipids of cells incubated with [1-<sup>14</sup>C] radiolabeled FA

Table 3 shows the FA composition of enterocytes and hepatocytes from the three fish species studied. Saturates, mainly represented by 16:0, was the most abundant group of FA (29.3–50.4%) in both cell types in all the species. Monounsaturated FA ranged between 13.7 and 28.9% of total FA, with about two-thirds being 18:1n-9. In enterocytes, total monounsaturated was slightly higher in *P. lascaris* (24.6% vs 13.7–16.3%). N-3 PUFA were an important group of FA in this cell type, remaining fairly stable among species (23.7–26.7%). 20:4n-6 and 20:5n-3 were more abundant in *S. salpa* (~15%) than in *P. lascaris* and *C. labrosus* (ranging between 2.5 and 5.9%) whereas 22:6n-3 was more relevant in *P. lascaris* (16.0  $\pm$  5.0%) and *C. labrosus* (18.4  $\pm$  4.9%) than in *S. salpa* (2.8  $\pm$  0.3%). Finally, 18:2n-6 represented between 3.5 and 7.7% of total FA in enterocytes from the three species. The FA composition of hepatocytes from *S. salpa* showed higher proportions of total n-3 PUFA, 20:5n-3, 22:5n-3 and 20:4n-6 than *P. lascaris* and *C. labrosus* while 22:6n-3 content was higher in hepatocytes from *C. labrosus* (12.3%) in comparison to *S. salpa* and *P. lascaris* (5.1% and 5.2%, respectively) (Table 3).

Table 4 shows the incorporation of radioactivity into TL of enterocytes and hepatocytes of the three species. Overall, both [1-<sup>14</sup>C] C<sub>18</sub> PUFA were generally the most incorporated FA in both cell types. Regardless of cell type and fish species, [1-<sup>14</sup>C] 22:6n-3 tended to be the least incorporated FA. *P. lascaris* presented the highest values of incorporation for all radiolabeled substrates in enterocytes, and for [1-<sup>14</sup>C] 18:3n-3 in hepatocytes. FA incorporation seems to be higher in hepatocytes than in enterocytes of *S. salpa*. By contrast, *P. lascaris* presented the opposite trend although [1-<sup>14</sup>C] 22:6n-3 did not differ between isolated cells (Table 4).

**Table 3**

Total lipid (mg lipid/mg protein) and main fatty acid composition (% of total FA) of control enterocytes and hepatocytes from *Sarpa salpa*, *Pegusa lascaris* and *Chelon labrosus*.

	<i>Sarpa salpa</i>		<i>Pegusa lascaris</i>		<i>Chelon labrosus</i>	
	Enterocytes	Hepatocytes	Enterocytes	Hepatocytes	Enterocytes	Hepatocytes
Total lipid	0.9 ± 0.2	3.0 ± 1.5	1.2 ± 0.0	1.8 ± 0.6	0.8 ± 0.2	2.2 ± 0.5
Total saturates <sup>1</sup>	29.3 ± 1.8	35.5 ± 1.3	37.3 ± 1.6	50.4 ± 8.2	36.7 ± 6.0	44.2 ± 2.0
14:0	0.8 ± 0.1	1.0 ± 0.1	1.4 ± 0.3	2.8 ± 1.1	1.4 ± 0.7	1.8 ± 0.3
16:0	17.0 ± 0.8	22.5 ± 1.6	19.0 ± 0.5	31.3 ± 6.8	16.1 ± 8.5	23.0 ± 2.6
18:0	11.4 ± 0.2	10.0 ± 1.0	13.9 ± 2.2	13.5 ± 2.8	14.3 ± 1.9	10.8 ± 0.9
Total monoenes <sup>1</sup>	13.7 ± 0.5	19.6 ± 4.9	24.6 ± 5.6	28.9 ± 9.8	16.3 ± 2.8	23.4 ± 6.9
16:1 <sup>2</sup>	1.9 ± 0.4	3.3 ± 2.5	2.6 ± 0.7	6.2 ± 2.0	2.0 ± 0.5	5.3 ± 3.8
18:1 <sup>3</sup>	10.2 ± 0.9	15.3 ± 3.6	19.9 ± 4.3	19.1 ± 6.1	13.1 ± 1.9	16.5 ± 3.0
20:1 <sup>3</sup>	0.7 ± 0.2	nd	0.2 ± 0.3	0.9 ± 0.4	0.7 ± 0.4	1.2 ± 0.9
Total n-6 PUFA <sup>1</sup>	22.9 ± 0.6	15.1 ± 1.3	8.9 ± 0.4	6.6 ± 2.0	16.3 ± 3.3	10.0 ± 3.6
18:2	3.5 ± 1.2	3.7 ± 0.7	4.0 ± 0.9	4.9 ± 3.0	7.7 ± 3.5	6.8 ± 2.1
18:3	nd	0.1 ± 0.2	nd	nd	nd	nd
20:3	1.4 ± 0.1	0.7 ± 0.1	nd	nd	nd	nd
20:4	14.9 ± 0.3	8.9 ± 1.6	2.5 ± 1.0	1.4 ± 0.6	5.9 ± 1.9	2.7 ± 1.4
22:5	0.7 ± 0.1	0.6 ± 0.1	1.2 ± 0.2	0.1 ± 0.2	1.2 ± 0.2	0.5 ± 0.1
Total n-3 PUFA <sup>1</sup>	25.2 ± 2.5	23.0 ± 4.1	23.7 ± 6.3	9.7 ± 4.9	26.7 ± 5.7	16.8 ± 6.1
18:3	0.9 ± 0.2	1.0 ± 0.2	0.6 ± 0.0	0.6 ± 0.0	1.2 ± 0.4	1.2 ± 0.2
20:5	15.1 ± 1.6	10.3 ± 2.4	3.4 ± 0.2	2.1 ± 1.2	4.6 ± 1.1	2.5 ± 1.1
22:5	5.8 ± 0.5	5.2 ± 1.4	3.5 ± 1.2	1.7 ± 1.1	1.9 ± 0.5	0.7 ± 0.3
22:6	2.8 ± 0.3	5.1 ± 1.5	16.0 ± 5.0	5.2 ± 2.6	18.4 ± 4.9	12.3 ± 4.8
n-3/n-6	1.1 ± 0.1	1.5 ± 0.2	2.7 ± 0.6	1.7 ± 1.2	1.7 ± 0.6	1.7 ± 0.2
20:4n-6/20:5n-3	1.0 ± 0.1	0.9 ± 0.2	0.7 ± 0.3	0.7 ± 0.2	1.3 ± 0.3	1.0 ± 0.2
22:6n-3/20:5n-3	0.2 ± 0.0	0.5 ± 0.2	4.7 ± 1.7	2.7 ± 0.4	4.1 ± 1.0	5.1 ± 1.2
Total n-3 LC-PUFA <sup>1</sup>	24.3 ± 2.6	21.5 ± 4.4	23.0 ± 6.0	9.0 ± 4.8	26.7 ± 5.7	15.6 ± 6.1

Results are presented as mean ± SD (*S. salpa*, n = 5; *P. lascaris*, n = 3; *C. labrosus*, n = 6). LC-PUFA, long chain polyunsaturated fatty acids (≥ C20 and ≥ 2 double bonds); nd, not detected.

<sup>1</sup> Includes some minor components not shown; <sup>2</sup> Mainly n-7 isomer; <sup>3</sup> Mainly n-9 isomer.

### 3.2. Bioconversion of radiolabeled FAs

Bioconversion of [<sup>1-14</sup>C] 18:2n-6, 18:3n-3 and 20:5n-3 in enterocytes and hepatocytes of the three fish species studied is shown in Table 5. Regardless of cellular type and species, the majority of radioactivity was consistently recovered as the unmodified substrate (59.1–92.3%). Nonetheless, enterocytes tended to show higher bioconversion rates (estimated as the sum of the products derived from each radiolabeled substrate) in both *S. salpa* (ranging from 10.6 to 37.0%) and *C. labrosus* (ranging from 10.3 to 37.6%) than in *P. lascaris* (ranging from 7.7 to 29.3%), with [<sup>1-14</sup>C] 20:5n-3 being the most modified FA (29.3–37.6%) in the three species (Table 5). Elongation was the most prominent activity over all substrates assayed in enterocytes from both *S. salpa* and *P. lascaris* and only over 20:5n-3 in *C. labrosus*. In addition, desaturation was registered exclusively towards [<sup>1-14</sup>C] 18:3n-3 in *S. salpa* and [<sup>1-14</sup>C] 18:2n-6 in *P. lascaris* (< 1%). On the other hand, products obtained from the action of both elongases and desaturases (E + D, elongation/desaturation) over the radiolabeled PUFA notably varied among substrates and species in this cellular type. Thus, E + D products from [<sup>1-14</sup>C] 20:5n-3 were significantly more

abundant than those from [<sup>1-14</sup>C] 18:3n-3 in *S. salpa*, whereas [<sup>1-14</sup>C] 18:2n-6 was the most modified substrate in *C. labrosus* (Table 5).

[<sup>1-14</sup>C] 20:5n-3 was also the most modified PUFA (22.5–40.9%) in hepatocytes except in *C. labrosus*, where [<sup>1-14</sup>C] 18:2n-6 was bio-converted to a similar extent (Table 5). Similarly to enterocytes, elongation was the most common activity over all substrates in hepatocytes from *P. lascaris* and *S. salpa* (8.1–32.1% and 8.7–17.4%, respectively), and additionally, over [<sup>1-14</sup>C] 20:5n-3 in *C. labrosus* (21.9 ± 3.4%). Desaturation was exclusively observed towards both [<sup>1-14</sup>C] C<sub>18</sub> PUFA in *S. salpa* and towards [<sup>1-14</sup>C] 18:2n-6 in *P. lascaris*, being in all cases < 3%. Moreover, E + D activity varied from 1.9 to 22.2% between substrates and species (Table 5). Thus, [<sup>1-14</sup>C] 18:2n-6 tended to be the most elongated and desaturated FA in hepatocytes from all species although only at a significant rate in *S. salpa*.

Desaturation over [<sup>1-14</sup>C] 18:3n-3 and [<sup>1-14</sup>C] 18:2n-6 in enterocytes from *S. salpa* and *P. lascaris*, respectively, led to the production of 18:4n-3 (0.3 ± 0.4%) and 18:3n-6 (1.0 ± 0.7%), respectively (Table 6). Although transformation of [<sup>1-14</sup>C] 18:2n-6 to 20:4n-6 was only present in *C. labrosus* (1.3 ± 0.4%), 22:5n-6 was detected in all species (Table 6). With respect to the n-3 series, both 20:5n-3 and

**Table 4**

Incorporation of radioactivity into total lipids (pmol mg prot<sup>-1</sup> h<sup>-1</sup>) of isolated enterocytes and hepatocytes of *Sarpa salpa*, *Pegusa lascaris* and *Chelon labrosus* incubated with [<sup>1-14</sup>C] 18:2n-6, [<sup>1-14</sup>C] 18:3n-3, [<sup>1-14</sup>C] 20:5n-3 and [<sup>1-14</sup>C] 22:6n-3.

[ <sup>1-14</sup> C] FA	Enterocytes				Hepatocytes			
	18:2n-6	18:3n-3	20:5n-3	22:6n-3	18:2n-6	18:3n-3	20:5n-3	22:6n-3
Species								
<i>Sarpa salpa</i>	90.5 ± 26.7 <sup>c</sup>	75.6 ± 26.0 <sup>bc</sup>	38.6 ± 19.7 <sup>ab</sup>	25.2 ± 10.7 <sup>a</sup>	154.7 ± 49.3	100.4 ± 37.9	71.2 ± 40.1	85.0 ± 49.5
<i>Pegusa lascaris</i>	471.4 ± 50.9 <sup>c</sup>	211.9 ± 7.3 <sup>b</sup>	127.6 ± 45.6 <sup>b</sup>	59.7 ± 19.8 <sup>a</sup>	142.2 ± 18.4 <sup>b</sup>	173.0 ± 12.5 <sup>b</sup>	54.3 ± 31.5 <sup>a</sup>	58.2 ± 4.9 <sup>a</sup>
<i>Chelon labrosus</i>	67.0 ± 16.3 <sup>b</sup>	67.5 ± 19.8 <sup>b</sup>	32.7 ± 13.8 <sup>a</sup>	12.3 ± 3.1 <sup>a</sup>	57.3 ± 35.3 <sup>b</sup>	88.5 ± 58.6 <sup>b</sup>	51.1 ± 25.4 <sup>b</sup>	10.7 ± 6.1 <sup>a</sup>

Values are presented as mean ± SD (*S. salpa*, n = 5, except for [<sup>1-14</sup>C] 22:6n-3, where n = 4; *P. lascaris*, n = 3; *C. labrosus*, n = 6). Different letters in superscript denote significant differences between [<sup>1-14</sup>C] FA for each cell type (p < .05).

**Table 5**

Bioconversions (% of total radioactivity) registered in isolated enterocytes and hepatocytes from *Sarpa salpa*, *Pegusa lascaris* and *Chelon labrosus* incubated with [ $1-^{14}\text{C}$ ] 18:2n-6, [ $1-^{14}\text{C}$ ] 18:3n-3 and [ $1-^{14}\text{C}$ ] 20:5n-3.

<i>Sarpa salpa</i>						
	Enterocytes			Hepatocytes		
[ $1-^{14}\text{C}$ ] PUFA	18:2	18:3	20:5	18:2	18:3	20:5
FA recovery	85.0 ± 5.0 <sup>b</sup>	89.4 ± 3.5 <sup>b</sup>	63.0 ± 2.8 <sup>a</sup>	80.8 ± 6.1 <sup>b</sup>	84.4 ± 2.0 <sup>b</sup>	68.0 ± 2.5 <sup>a</sup>
Elongation	10.5 ± 5.3 <sup>a</sup>	8.1 ± 4.0 <sup>a</sup>	20.8 ± 3.3 <sup>b</sup>	8.7 ± 3.8 <sup>a</sup>	9.7 ± 3.5 <sup>a</sup>	17.4 ± 1.7 <sup>b</sup>
Desaturation	nd	0.3 ± 0.4	nd	1.7 ± 0.4	2.3 ± 1.0	nd
E + D	2.4 ± 1.4 <sup>ab</sup>	0.5 ± 0.7 <sup>a</sup>	2.8 ± 1.2 <sup>b</sup>	7.0 ± 2.5 <sup>b</sup>	3.5 ± 1.8 <sup>a</sup>	1.9 ± 0.8 <sup>a</sup>
<i>De novo</i>	1.9 ± 0.2 <sup>a</sup>	1.2 ± 0.6 <sup>a</sup>	12.8 ± 3.9 <sup>b</sup>	1.2 ± 0.2 <sup>a</sup>	nd	10.0 ± 3.8 <sup>b</sup>
Unknown	0.2 ± 0.2	0.5 ± 0.2	0.5 ± 1.1	0.6 ± 0.8	nd	2.6 ± 1.9
<i>Pegusa lascaris</i>						
	Enterocytes			Hepatocytes		
[ $1-^{14}\text{C}$ ] PUFA	18:2	18:3	20:5	18:2	18:3	20:5
FA recovery	87.0 ± 1.8 <sup>b</sup>	92.3 ± 3.1 <sup>b</sup>	70.7 ± 5.1 <sup>a</sup>	80.6 ± 5.0 <sup>b</sup>	89.3 ± 3.2 <sup>b</sup>	59.1 ± 8.6 <sup>a</sup>
Elongation	9.6 ± 0.9 <sup>a</sup>	6.8 ± 2.7 <sup>a</sup>	21.1 ± 1.0 <sup>b</sup>	13.3 ± 3.4 <sup>a</sup>	8.1 ± 4.2 <sup>a</sup>	32.1 ± 7.2 <sup>b</sup>
Desaturation	1.0 ± 0.7	nd	nd	2.0 ± 0.7	nd	nd
E + D	2.2 ± 0.6	0.8 ± 0.7	4.6 ± 5.9	3.5 ± 1.1 <sup>b</sup>	1.6 ± 0.5 <sup>a</sup>	2.7 ± 0.3 <sup>ab</sup>
<i>De novo</i>	nd	nd	3.6 ± 4.5	nd	1.0 ± 1.7	6.1 ± 3.7
Unknown	0.2 ± 0.1	0.1 ± 0.2	nd	0.5 ± 1.0	nd	nd
<i>Chelon labrosus</i>						
	Enterocytes			Hepatocytes		
[ $1-^{14}\text{C}$ ] PUFA	18:2	18:3	20:5	18:2	18:3	20:5
FA recovery	83.9 ± 2.8 <sup>b</sup>	89.7 ± 0.6 <sup>c</sup>	62.4 ± 2.0 <sup>a</sup>	66.4 ± 14.4 <sup>a</sup>	92.2 ± 1.6 <sup>b</sup>	77.5 ± 4.3 <sup>a</sup>
Elongation	4.0 ± 1.0 <sup>a</sup>	4.5 ± 1.2 <sup>a</sup>	28.4 ± 1.2 <sup>b</sup>	9.5 ± 9.4 <sup>ab</sup>	2.0 ± 1.9 <sup>a</sup>	21.9 ± 3.4 <sup>b</sup>
Desaturation	nd	nd	nd	nd	nd	nd
E + D	5.4 ± 0.9 <sup>b</sup>	3.5 ± 0.9 <sup>a</sup>	nd	22.2 ± 13.8	5.5 ± 1.6	nd
<i>De novo</i>	5.6 ± 0.7 <sup>b</sup>	nd	0.3 ± 0.4 <sup>a</sup>	1.8 ± 2.8	0.3 ± 0.6	nd
Unknown	1.1 ± 1.2	2.3 ± 0.5	8.9 ± 2.2	nd	nd	0.6 ± 1.0

Values are presented as mean ± SD (*S. salpa*, n = 5; *P. lascaris*, n = 3; *C. labrosus*, n = 6). E + D, elongation and desaturation; nd, not detected. *De novo*: shorter FAs produced by using the [ $1-^{14}\text{C}$ ] released after a first  $\beta$ -oxidation cycle of the radiolabeled substrate. Different letters in superscript denote significant differences between [ $1-^{14}\text{C}$ ] fatty acids for each cell type (p < .05).

**Table 6**

Products obtained (% of total radioactivity) from the incubation of isolated enterocytes and hepatocytes with [ $1-^{14}\text{C}$ ] 18:2n-6, [ $1-^{14}\text{C}$ ] 18:3n-3 and [ $1-^{14}\text{C}$ ] 20:5n-3

	Enterocytes			Hepatocytes		
	<i>S. salpa</i>	<i>P. lascaris</i>	<i>C. labrosus</i>	<i>S. salpa</i>	<i>P. lascaris</i>	<i>C. labrosus</i>
<b>[<math>1-^{14}\text{C}</math>] 18:2n-6</b>						
18:3	nd	1.0 ± 0.7	nd	1.7 ± 0.4	2.0 ± 0.7	nd
20:2	8.0 ± 5.2	8.3 ± 1.2	2.0 ± 0.5	7.2 ± 3.4	12.2 ± 0.8	4.4 ± 4.2
20:3	nd	0.4 ± 0.3	nd	0.9 ± 0.9	0.3 ± 0.5	nd
20:4	nd	nd	1.3 ± 0.4	0.4 ± 0.5	nd	9.9 ± 6.7
22:2	2.6 ± 0.8	1.3 ± 0.9	1.9 ± 0.6	1.5 ± 1.0	1.1 ± 1.9	5.1 ± 5.2
22:4	1.2 ± 0.3	nd	0.8 ± 0.4	1.2 ± 1.2	nd	nd
22:5	1.3 ± 1.1	1.5 ± 1.0	3.3 ± 0.5	4.6 ± 1.9	3.2 ± 1.1	12.3 ± 7.2
24:5	nd	0.3 ± 0.6	nd	nd	nd	nd
<b>[<math>1-^{14}\text{C}</math>] 18:3n-3</b>						
18:4	0.3 ± 0.4	nd	nd	2.3 ± 1.0	nd	nd
20:3	7.2 ± 3.5	6.5 ± 2.9	1.5 ± 0.4	8.8 ± 4.0	8.1 ± 4.2	2.0 ± 1.9
20:4	nd	nd	1.5 ± 0.4	1.0 ± 0.3	nd	3.3 ± 3.2
20:5	nd	0.3 ± 0.2	0.8 ± 0.3	nd	1.2 ± 0.4	0.8 ± 0.7
22:3	1.0 ± 0.9	0.2 ± 0.4	0.9 ± 0.5	0.9 ± 0.9	nd	nd
22:5	nd	nd	0.1 ± 0.2	0.4 ± 0.4	nd	nd
22:6	nd	0.5 ± 0.5	1.2 ± 0.3	0.9 ± 0.3	0.4 ± 0.7	1.4 ± 1.2
24:3	nd	nd	0.9 ± 0.5	nd	nd	nd
24:6	0.5 ± 0.7	nd	nd	1.2 ± 1.1	nd	nd
<b>[<math>1-^{14}\text{C}</math>] 20:5n-3</b>						
22:5	15.3 ± 2.6	12.7 ± 1.7	15.0 ± 0.3	14.6 ± 1.2	23.3 ± 4.4	12.4 ± 3.5
22:6	nd	4.6 ± 5.9	nd	nd	2.7 ± 0.3	nd
24:5	5.6 ± 2.1	8.4 ± 2.6	4.1 ± 0.7	2.8 ± 0.8	8.7 ± 4.3	4.9 ± 2.9
24:6	2.8 ± 1.2	nd	nd	1.9 ± 0.8	nd	nd

Values are presented as mean ± SD (*S. salpa*, n = 5; *P. lascaris*, n = 3; *C. labrosus*, n = 6). nd, not detected.

22:6n-3 were obtained from [ $1-^{14}\text{C}$ ] 18:3n-3 in *P. lascaris* ( $0.3 \pm 0.2$  and  $0.5 \pm 0.5\%$ , respectively) and *C. labrosus* ( $0.8 \pm 0.3$  and  $1.2 \pm 0.3\%$ , respectively) but not in *S. salpa*. However, only *P. lascaris* was able to synthesize 22:6n-3 from [ $1-^{14}\text{C}$ ] 20:5n-3 ( $4.6 \pm 5.9\%$ ) (Table 6).

Furthermore, 20:4n-6 was produced from [ $1-^{14}\text{C}$ ] 18:2n-6 in hepatocytes from both *S. salpa* ( $0.4 \pm 0.5\%$ ) and *C. labrosus* ( $9.9 \pm 6.7\%$ ). In addition, [ $1-^{14}\text{C}$ ] 18:3n-3 was bioconverted in a similar pattern as described above for enterocytes. More specifically, both 20:5n-3 and 22:6n-3 were obtained from [ $1-^{14}\text{C}$ ] 18:3n-3 in *P. lascaris* ( $1.2 \pm 0.4\%$  and  $0.4 \pm 0.7\%$ , respectively) and *C. labrosus* ( $0.8 \pm 0.7$  and  $1.4 \pm 1.2\%$ , respectively), whereas only 22:6n-3 was detected in *S. salpa* ( $0.9 \pm 0.3\%$ ). Besides, only *P. lascaris* synthesize 22:6n-3 from [ $1-^{14}\text{C}$ ] 20:5n-3 (Table 6).

### 3.3. *Elovl5* sequences, phylogenetics, functional characterization and tissue expression

*Elovl5* elongase from *S. salpa*, *P. lascaris* and *C. labrosus* consist of an ORF of 885, 867 and 876 bp, encoding putative proteins of 295, 289 and 292 aa, respectively. The newly cloned *elovl5* cDNA sequences were deposited in the GenBank database under the accession numbers MT019561, MT019562 and MT019563. Our phylogenetic analysis showed that the three elongases clustered together within a branch containing *Elovl5* from vertebrates, itself separated from other PUFA elongases, namely *Elovl2* and *Elovl4* (Fig. 2). These results confirm that the sequences investigated herein are all *Elovl5* elongases.

The putative proteins encoded by the *elovl5* cDNA sequences were functionally characterized in yeast. Our results show that the three *Elovl5* had activity over all  $\text{C}_{18}$  and  $\text{C}_{20}$  PUFA substrates assayed (Table 7). With the exception of *Elovl5* in *P. lascaris* which exhibited a remarkably low activity towards 22:5n-3, the herein functionally characterized *Elovl5* did not have the capacity to elongate  $\text{C}_{22}$  PUFA substrates (Table 7).

The highest expression of *elovl5* in both *S. salpa* and *P. lascaris* was observed in liver, gut and brain whereas in *C. labrosus*, brain presented the highest expression ratio, and liver and gill the lowest ones (Fig. 3).

## 4. Discussion

The ability of fish to biosynthesize LC-PUFA is one of the factors to be considered to determine the potential interest of a particular species as candidate for the diversification of aquaculture. Thus, it could allow for both the development of feedstuff formulations optimized for the target species as well as the selection of fish with high capacity to utilize  $\text{C}_{18}$  fatty acid precursors from dietary VO while maintaining proper growth and development, and its nutritional quality in terms of flesh n-3 LC-PUFA content.

In the present work, the incorporation of radioactivity into total lipids of isolated cells from the three fish species studied (*S. salpa*, *P. lascaris* and *C. labrosus*) showed notable differences between [ $1-^{14}\text{C}$ ]  $\text{C}_{18}$  PUFA precursors (18:2n-6 and 18:3n-3) and [ $1-^{14}\text{C}$ ] LC-PUFA (20:5n-3 and 22:6n-3). Overall, both enterocytes and hepatocytes seem to preferentially incorporate  $\text{C}_{18}$  precursors, followed by 20:5n-3 and finally 22:6n-3 (Table 4), in spite of the reported physiological importance of these two LC-PUFA. A similar pattern was found in juvenile of *S. aurata* (Mourete and Tocher, 1993a). However, due to results obtained in a subsequent study in *S. aurata*, together with studies in *L. aurata* and *Scophthalmus maximus* (Linares and Henderson, 1991; Mourete and Tocher, 1993b, 1994), a preferential retention of 20:5n-3 in marine fish was proposed (Mourete and Tocher, 1994). A lower affinity of proteins involved in FA membrane translocation processes for LC-PUFA and a poorer ability of  $\geq \text{C}_{20}$  PUFA to diffuse through cell membranes (Pérez et al., 1999) may be responsible for the observed incorporation differences. In addition, although  $\beta$ -oxidation measurement was not carried out in our study due to sample limitation, a preferential  $\beta$ -oxidation

activity over  $\text{C}_{18}$  precursors could not be ruled out since  $\text{C}_{18}$  PUFA are readily oxidized substrates, in comparison with LC-PUFA, which are mostly preserved and stored in tissue membranes (Almáida-Pagán et al., 2007; Mourete et al., 2005). Thus, the apparent affinity for  $\text{C}_{18}$  PUFA in the studied species may be due either, to the ability of cells to more easily incorporate FA with shorter chains ( $\text{C}_{18}$  vs.  $\geq \text{C}_{20-22}$ ) or to their preference to be  $\beta$ -oxidized.

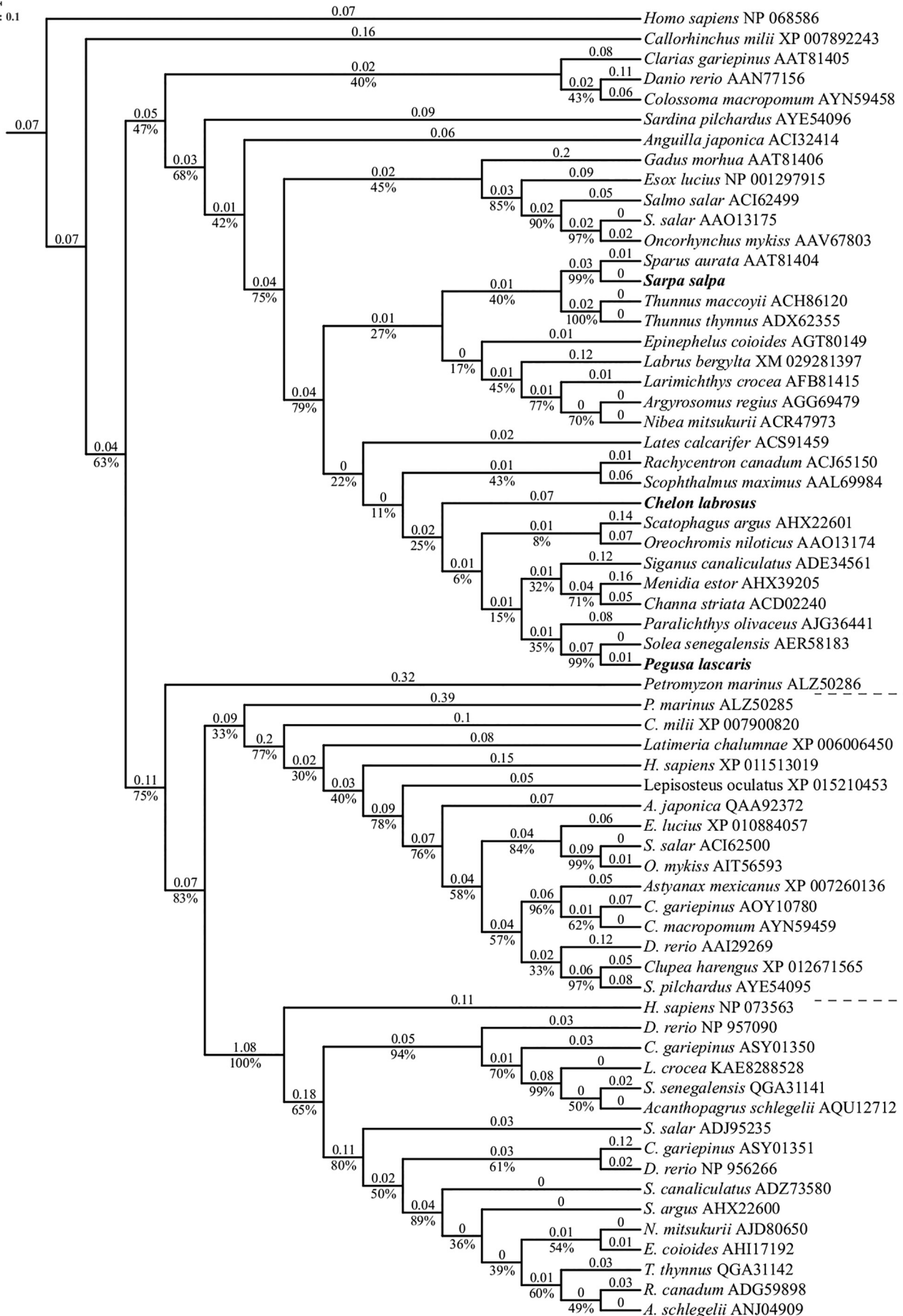
Regardless of the species, bioconversion rates in enterocytes and hepatocytes ranged between 7.7 and 40.9% (Table 5), showing higher bioconversion capacities than other teleosts previously studied such as *S. aurata*, *S. maximus* or *S. senegalensis* (Díaz-López et al., 2010; Morais et al., 2015; Rodríguez et al., 2002). Moreover, as it has been previously reported in *S. maximus* and *S. senegalensis* (Morais et al., 2015; Rodríguez et al., 2002), 20:5n-3 is the most modified FA, mainly elongated by *Elovl5* action, in the enterocytes of the three species, and in the hepatocytes of *S. salpa* and *P. lascaris*. In spite of this, 22:6n-3 from [ $1-^{14}\text{C}$ ] 20:5n-3 was only detected in *P. lascaris* (Table 6), probably due to the  $\Delta 4$  activity described before (Garrido et al., 2019), although the Sprecher route may not be completely ruled out in this species, as it will be further discussed in this work.

Our recent previous results (Garrido et al., 2019) demonstrated the existence of a *Fads2* with  $\Delta 6$  and  $\Delta 8$  activities in *S. salpa* by heterologous expression in yeast. Therefore, the presence of 18:4n-3 and 24:6n-3 in both enterocytes and hepatocytes of *S. salpa* incubated with [ $1-^{14}\text{C}$ ] 18:3n-3 agrees well with the  $\Delta 6$  activity above mentioned, although for incubations with [ $1-^{14}\text{C}$ ] 18:2n-6 this activity was found exclusively in hepatocytes (Table 6). Also in agreement with our results on *S. salpa*, the  $\Delta 6$  activity for *Fads2* towards both 18:3n-3 and 24:5n-3 has also been observed in *S. aurata* using radioactivity-based assays and yeast expression systems (Mourete and Tocher, 1993a; Oboh et al., 2017; Tocher and Ghioni, 1999). Moreover, as reported herein for *S. salpa*, 18:3n-6 but not 24:5n-6 was detected in *S. aurata* *in vivo* assays or when fibroblasts were incubated with [ $1-^{14}\text{C}$ ] 18:2n-6 (Mourete and Tocher, 1993a; Tocher and Ghioni, 1999). Our present results in *S. salpa* add more evidences to the possible conservation of the  $\Delta 6$  desaturase capacity among members of the Sparidae family as previously reported in *S. aurata*. In addition, the presence of 20:3n-6 and 20:4n-3 in hepatocytes (Table 6), confirms the  $\Delta 8$  activity recently suggested by our results using molecular tools (Garrido et al., 2019). A  $\Delta 5$  desaturation activity was also detected in hepatocytes of *S. salpa*, obtaining 20:4n-6 from the incubation with [ $1-^{14}\text{C}$ ] 18:2n-6. Activities, which have been also reported in *S. aurata*, together with the presence of trace levels of 20:5n-3. Thus, it is possible that *Fads2* had also some  $\Delta 6/\Delta 5$  activity in these sparids. Finally, 22:6n-3 was only detected in hepatocytes incubated with [ $1-^{14}\text{C}$ ] 18:3n-3 but not with [ $1-^{14}\text{C}$ ] 20:5n-3. The lower total incorporation of [ $1-^{14}\text{C}$ ] 20:5n-3 compared to [ $1-^{14}\text{C}$ ] 18:3n-3 in *S. salpa*, may explain these differences of bioconversion rates between substrates.

*S. salpa* displayed elongation activity in both the radiolabeled assays and in the functional characterization of *Elovl5* by heterologous expression in yeast, obtaining  $\text{C}_{20}$  and  $\text{C}_{22}$  products from the  $\text{C}_{18}$  and  $\text{C}_{20}$  precursors, respectively (Tables 6, 7). *Elovl5* is known to mainly act over  $\text{C}_{18}$  and  $\text{C}_{20}$  substrates as indicated by heterologous expression in yeast (Monroig et al., 2012). Furthermore, elongation activity over  $\text{C}_{22}$  PUFA was also observed in our study when cells were incubated with [ $1-^{14}\text{C}$ ] 20:5n-3 according to what has been reported in *S. aurata* (Agaba et al., 2005). Collectively, our results indicate that both *S. salpa* and *S. aurata* have a rather similar capacity for LC-PUFA biosynthesis despite the remarkably different trophic level of these two sparid species.

*P. lascaris* enterocytes and hepatocytes displayed similar lipid metabolic characteristics.  $\text{C}_{20}$ ,  $\text{C}_{22}$  and  $\text{C}_{24}$  FAs were detected as elongation products when both cell types were incubated in the presence of [ $1-^{14}\text{C}$ ]  $\text{C}_{18}$  and [ $1-^{14}\text{C}$ ]  $\text{C}_{20}$  substrates, in accordance to the *Elovl5* activities detected in yeast (Tables 6, 7), and as reported by Morais et al. (2012) in its phylogenetically close *S. senegalensis*. At the same time, multiple

Tree scale: 0.1



Elov15

Elov12

Elov14

(caption on next page)

**Fig. 2.** Phylogenetic tree of *elovl5* using the deduced amino acid sequences from *Sarpa salpa*, *Pegusa lascaris* and *Chelon labrosus*. The number over horizontal branch length shows the branch lengths which is proportional to the amino acid substitution rate per site, whereas the percentage number under the horizontal branch length is the bootstrap replicates from 1000 iterations.

**Table 7**

Percentage of conversion of fatty acid (FA) substrates exogenously added to transgenic yeast (*Saccharomyces cerevisiae*) transformed with the coding region of *elovl5* from *Sarpa salpa*, *Pegusa lascaris* and *Chelon labrosus*.

FA substrate	FA product	% conversion		
		<i>Sarpa salpa</i>	<i>Pegusa lascaris</i>	<i>Chelon labrosus</i>
18:2n-6	20:2n-6	5.1	29.6	15.2
18:3n-3	20:3n-3	29.3	44.7	42.0
18:3n-6	20:3n-6	38.3	81.6	58.4
18:4n-3	20:4n-3	50.2	80.3	64.4
20:4n-6	22:4n-6	30.2	36.1	27.0
20:5n-3	22:5n-3	75.7	70.8	69.1
22:4n-6	24:4n-6	nd	nd	nd
22:5n-3	24:5n-3	nd	2.3	nd

Results are expressed as a percentage of total fatty acid substrate converted to elongated product. nd, not detected.

products of desaturation were identified with our experimental design. On one hand, the presence of 22:5n-6 from [ $1-^{14}C$ ] 18:2n-6 as well as that of 22:6n-3 when incubating with [ $1-^{14}C$ ] 18:3n-3 and [ $1-^{14}C$ ] 20:5n-3 (Fig. 1) in both cell types could confirm the  $\Delta 4$  activity previously reported by our group with a molecular approach (Garrido et al., 2019). Nevertheless, these results seem to indicate that this species could have another Fads2 with  $\Delta 6/\Delta 5$  activity still uncharacterized. On the other hand, our radioactive assays suggest the existence of  $\Delta 6$  and  $\Delta 8$  activities when incubating with [ $1-^{14}C$ ] 18:2n-6, based on the detection of 18:3n-6 and 20:3n-6, as well as 24:5n-6 in enterocytes (Table 6). While similar bioconversions were not registered when using [ $1-^{14}C$ ] 18:3n-3 as substrate, the transformations towards [ $1-^{14}C$ ] 18:2n-6 indicate that *P. lascaris* may possess, along with the  $\Delta 4$  Fads2 previously alluded (Garrido et al., 2019), a second Fads2 with  $\Delta 6/\Delta 8$  activities, and a possible residual  $\Delta 6/\Delta 5$  activity as Morais et al. (2015) suggested in *S. senegalensis*. What is more, perhaps a n-6 preference/specificity could be the reason why Morais et al. (2015) did not find  $\Delta 6$  activity in *S. senegalensis*, since only [ $1-^{14}C$ ] 18:3n-3 and [ $1-^{14}C$ ] 20:5n-3 were used as substrates. Importantly, these results suggest that *P. lascaris* seems to be able to biosynthesize 22:6n-3 via two different

routes, namely the  $\Delta 4$  pathway operated by the functionally characterized Fads2 (Garrido et al., 2019), and the Sprecher pathway operated by a yet uncharacterized Fads2.

The enzymatic activity assays carried out on *C. labrosus* enterocytes and hepatocytes demonstrated that this species has  $\Delta 8$  and  $\Delta 5$  desaturase capacities, as well as the ability to biosynthesize 22:6n-3 from [ $1-^{14}C$ ] 18:3n-3 (Table 6). Although the  $\Delta 8$  desaturase activity was demonstrated in the  $\Delta 6/\Delta 8$  Fads2 characterized in our earlier study on *C. labrosus* (Garrido et al., 2019), no activity as  $\Delta 5$  desaturase was detected through molecular tools for that enzyme. Therefore, the present study performed in isolated cells suggest that *C. labrosus* has extra copies of Fads2, possibly containing  $\Delta 5$  desaturation capacity. Consequently, the coexistence of  $\Delta 5$ ,  $\Delta 6$  and  $\Delta 8$  activities within *C. labrosus* may account for all the desaturation reactions required for the bioconversion of 18:3n-3 to 22:6n-3 detected in our experiments. 22:6n-3 biosynthesis seemed to be performed by the Sprecher pathway as it has been previously described for *L. aurata* (Mourente and Tocher, 1993b). However, as  $C_{24}$  intermediaries of the Sprecher pathway were not detected in the enzymatic assays (Table 6), the  $\Delta 4$  pathway cannot be completely ruled out. Fads2 with  $\Delta 4$  activity has not been yet characterized in the Mugilidae family, but it has been demonstrated in other families from the same lineage Ovalentaria, such as Cichlidae or Atherinidae (Fonseca-Madrigal et al., 2014; Garrido et al., 2019; Oboh et al., 2017). 22:6n-3 is biosynthesized from [ $1-^{14}C$ ] 18:3n-3 but not from [ $1-^{14}C$ ] 20:5n-3 in *C. labrosus*. In *S. salar*, the addition of 20:5n-3 inhibited LC-PUFA biosynthesis in cells lines (AS) (Zheng et al., 2009b), while increasing doses of 20:5n-3 decreased the  $\Delta 5$  and  $\Delta 6$  gene expression in the same species Kjær et al. (2016). This, together with the lower incorporation into total lipid of [ $1-^{14}C$ ] 20:5n-3 vs. [ $1-^{14}C$ ] 18:3n-3, could account for the differences found between both substrates (Table 4).

Both the functional characterization of Elov15 in yeast and radiolabeled assays with isolated cells showed elongation from  $C_{18}$  and  $C_{20}$  precursors to  $C_{20}$  and  $C_{22}$  products (Tables 6 and 7), respectively, in *C. labrosus*. The detection of 24:5n-3 when both cell types were incubated with [ $1-^{14}C$ ] 20:5n-3 could indicate the action of other Elov1, such as Elov14, which is able to elongate a range of PUFA substrates including 22:5n-3 (Monroig et al., 2011b, 2012).

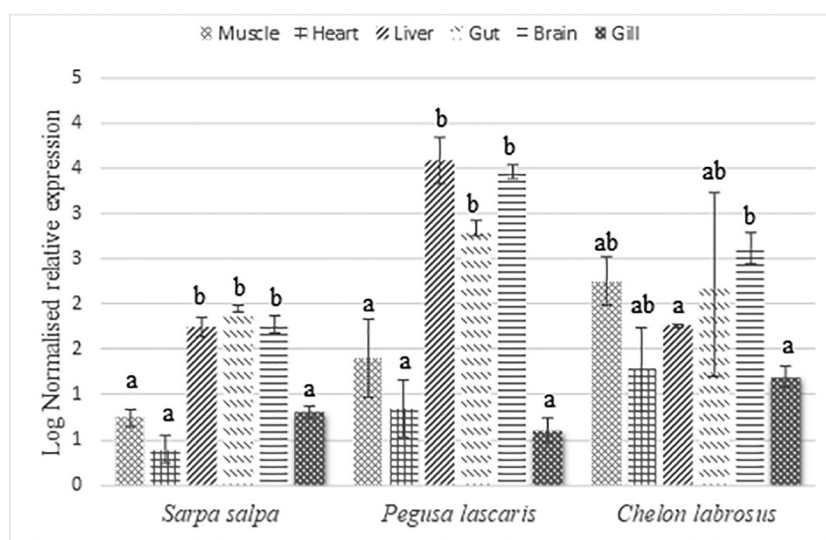


**Fig. 3.** Tissue distribution of *elovl5* in *Sarpa salpa*, *Pegusa lascaris* and *Chelon labrosus*. Data are presented as geometric mean log normalized expression ratios  $\pm$  standard errors (*S. salpa* and *P. lascaris* n = 4; *C. labrosus*, n = 3). Different letters denote significant differences among tissue for each specie (p < .05).

The gene expression pattern of *elovl5* varied among species. *S. salpa* and *P. lascaris* had the highest number of transcripts in the liver, gut and brain, while this occurred in the brain of *C. labrosus*, where liver and gill showed the lowest expression (Fig. 3). Until now, the differences in tissue gene expression distribution have been hypothesized to be associated to the origin of the species (marine or freshwater) (Kabeya et al., 2017). Furthermore, it is known that different factors such as nutritional history, developmental stage, etc., can affect the tissue distribution patterns of *elovl5* (Monroig et al., 2018). Besides gut and liver, a few evidences suggest that other tissues can also biosynthesize LC-PUFA. In this sense, the brain is a conservative tissue rich in LC-PUFA and therefore, a higher number of transcripts could be necessary in order to satisfy an optimal level of LC-PUFA for proper function (Zheng et al., 2009a).

It has been hypothesized that fish occupying low trophic levels, require only C<sub>18</sub> PUFA in the diet, being capable of *de novo* biosynthesize LC-PUFA, while those with high trophic levels, are unable to form LC-PUFA from C<sub>18</sub> precursors and therefore need a dietary supply of LC-PUFA. Nonetheless, fish occupying intermediate trophic level, which may require either C<sub>18</sub> PUFA or LC-PUFA depending on their ecological niche and life history, called into question this generalization (Trushenski and Rombenso, 2019). Our results obtained in three fish species with different trophic level, indicate that this factor might not be a good indicator for LC-PUFA biosynthesis.

In conclusion, phylogeny of the fish species, instead of trophic level, might be a more relevant factor in the LC-PUFA biosynthetic capacity. *S. salpa* and *P. lascaris* showed lipid metabolism characteristics similar to two established commercial species such as *S. aurata* and *S. senegalensis*, respectively, and could be adequate candidates for aquaculture diversification. The LC-PUFA biosynthetic capacity of wild *S. salpa*, *P. lascaris* and *C. labrosus* resembled that of their phylogenetically close species *S. aurata*, *S. senegalensis* and *L. aurata*, respectively. The desaturase activities observed in this study include Δ5, Δ6 and Δ8 activities in *S. salpa*, Δ5 and Δ8 activity in *C. labrosus*, and Δ6/Δ5 residual activity and Δ4 in *P. lascaris*. Thus, confirming the ability of the three species studied to biosynthesize 22:6n-3 from 18:3n-3.

#### Declaration of competing interest

The authors declare that they have no known competing financial interests or personal relationships that could have appeared to influence the work reported in this paper.

#### Acknowledgments

This study was funded by Ministerio de Economía y Competitividad (AGL2015-70994-R). A. Galindo and M. Marrero are supported by a PhD grant by Cajasiete and Gobierno de Canarias, respectively. Dr. Covadonga Rodríguez and Dr. Ana Bolaños are members of the Instituto de Tecnologías Biomédicas de Canarias (ITB). We also thank Dr. Inmaculada Giráldez from Universidad de Huelva for her assistance with laboratory facilities and Dr. Deiene Rodríguez-Barreto for her useful revision and assistance with the manuscript.

#### Appendix A. Supplementary data

Supplementary data to this article can be found online at <https://doi.org/10.1016/j.aquaculture.2020.735761>.

#### References

Agaba, M.K., Tocher, D.R., Zheng, X., Dickson, C.A., Dick, J.R., Teale, A.J., 2005. Cloning and functional characterisation of polyunsaturated fatty acid elongases of marine and freshwater teleost fish. *Comp. Biochem. Physiol. B Biochem. Mol. Biol.* 142, 342–352.

Almolda-Pagán, P.F., Hernández, M.D., García García, B., Madrid, J.A., De Costa, J., Mendiola, P., 2007. Effects of total replacement of fish oil by vegetable oils on n-3

and n-6 polyunsaturated fatty acid desaturation and elongation in sharpnose seabream (*Diplodus puntazzo*) hepatocytes and enterocytes. *Aquaculture* 272, 589–598.

Bell, M.V., Tocher, D.R., 2009. Biosynthesis of polyunsaturated fatty acids in aquatic ecosystems: general pathways and new directions. In: Kainz, M., Brett, M.T., Arts, M.T. (Eds.), *Lipids in Aquatic Ecosystems*. Springer New York, New York, NY, pp. 211–236.

Capella-Gutiérrez, S., Silla-Martínez, J.M., Gabaldón, T., 2009. trimAl: a tool for automated alignment trimming in large-scale phylogenetic analyses. *Bioinformatics* 25, 1972–1973.

Castro, L.F.C., Tocher, D.R., Monroig, Ó., 2016. Long-chain polyunsaturated fatty acid biosynthesis in chordates: insights into the evolution of fads and Elov1 gene repertoire. *Prog. Lipid Res.* 62, 25–40.

Christie, W.W., Han, X., 2010. *Lipid Analysis: Isolation, Separation, Identification and Lipidomic Analysis*. Oily Press, an imprint of P.J. Barnes & Associates, pp. 55–66.

Darriba, D., Posada, D., Kozlov, A.M., Stamatakis, A., Morel, B., Flouri, T., 2020. ModelTest-NG: a new and scalable tool for the selection of DNA and protein evolutionary models. *Mol. Biol. Evol.* 37, 291–294.

Díaz-López, M., Pérez, M.J., Acosta, N.G., Jerez, S., Dorta-Guerra, R., Tocher, D.R., Lorenzo, A., Rodríguez, C., 2010. Effects of dietary fish oil substitution by Echium oil on enterocyte and hepatocyte lipid metabolism of gilthead seabream (*Sparus aurata* L.). *Comp. Biochem. Physiol. B Biochem. Mol. Biol.* 155, 371–379.

FAO, 2018. *The State of World Fisheries and Aquaculture 2018: Meeting the Sustainable Development Goals*. Rome. Licence: CC BY-NC-SA 3.0 IGO.

Folch, J., Lees, M., Sloane-Stanley, G.H., 1957. A simple method for the isolation and purification of total lipides from animal tissues. *J. Biol. Chem.* 226, 497–509.

Fonseca-Madrugal, J., Navarro, J.C., Hontoria, F., Tocher, D.R., Martínez-Palacios, C.A., Monroig, Ó., 2014. Diversification of substrate specificities in teleostei Fads2: characterization of Δ4 and Δ6Δ5 desaturases of *Chirostoma estor*. *J. Lipid Res.* 55, 1408–1419.

Garlito, B., Portoles, T., Niessen, W.M.A., Navarro, J.C., Hontoria, F., Monroig, Ó., Varó, I., Serrano, R., 2019. Identification of very long-chain (> C24) fatty acid methyl esters using gas chromatography coupled to quadrupole/time-of-flight mass spectrometry with atmospheric pressure chemical ionization source. *Anal. Chim. Acta* 1051, 103–109.

Garrido, D., Kabeya, N., Betancor, M.B., Pérez, J.A., Acosta, N.G., Tocher, D.R., Rodríguez, C., Monroig, Ó., 2019. Functional diversification of teleost Fads2 fatty acyl desaturases occurs independently of the trophic level. *Sci. Rep.* 9, 11199.

Garrido, D., Monroig, Ó., Galindo, A., Betancor, M.B., Perez, J.A., Kabeya, N., Marrero, M., Rodríguez, C., 2020. Lipid metabolism in *Tinca tinca* and its n-3 LC-PUFA biosynthesis capacity. *Aquaculture* 523, 735147.

Hastings, N., Agaba, M., Tocher, D.R., Leaver, M.J., Dick, J.R., Sargent, J.R., Teale, A.J., 2001. A vertebrate fatty acid desaturase with Delta 5 and Delta 6 activities. *Proc. Natl. Acad. Sci. U. S. A.* 98, 14304–14309.

Kabeya, N., Chiba, M., Haga, Y., Satoh, S., Yoshizaki, G., 2017. Cloning and functional characterization of fads2 desaturase and elov15 elongase from Japanese flounder *Paralichthys olivaceus*. *Comp. Biochem. Physiol. B Biochem. Mol. Biol.* 214, 36–46.

Kabeya, N., Yezzelman, S., Oboh, A., Tocher, D.R., Monroig, Ó., 2018. Essential fatty acid metabolism and requirements of the cleaner fish, ballan wrasse *Labrus bergylla*: defining pathways of long-chain polyunsaturated fatty acid biosynthesis. *Aquaculture* 488, 199–206.

Katoh, K., Rozewicki, J., Yamada, K.D., 2019. MAFFT online service: multiple sequence alignment, interactive sequence choice and visualization. *Brief. Bioinform.* 20, 1160–1166.

Kjær, M.A., Ruyter, B., Berge, G.M., Sun, Y., Østbye, T.-K.K., 2016. Regulation of the omega-3 fatty acid biosynthetic pathway in Atlantic salmon hepatocytes. *PLoS One* 11, e0168230.

Kuah, M.-K., Jaya-Ram, A., Shu-Chien, A.C., 2015. The capacity for long-chain polyunsaturated fatty acid synthesis in a carnivorous vertebrate: functional characterisation and nutritional regulation of a Fads2 fatty acyl desaturase with Δ4 activity and an Elov15 elongase in striped snakehead (*Channa striata*). *Biochim. Biophys. Acta Mol. Cell Biol. Lipids* 1851, 248–260.

Lee, J., Lee, H., Kang, S., Park, W., 2016. Fatty acid desaturases, polyunsaturated fatty acid regulation, and biotechnological advances. *Nutrients* 8, 23.

Letunic, I., Bork, P., 2016. Interactive tree of life (iTOL) v3: an online tool for the display and annotation of phylogenetic and other trees. *Nucleic Acids Res.* 44, W242–W245.

Li, Y., Monroig, Ó., Zhang, L., Wang, S., Zheng, X., Dick, J.R., You, C., Tocher, D.R., 2010. Vertebrate fatty acyl desaturase with Δ4 activity. *Proc. Natl. Acad. Sci. U. S. A.* 107, 16840–16845.

Linares, F., Henderson, R.J., 1991. Incorporation of <sup>14</sup>C-labelled polyunsaturated fatty acids by juvenile turbot, *Scophthalmus maximus* (L.) in vivo. *J. Fish Biol.* 38, 335–347.

Lowry, O.H., Rosebrough, N.J., Farr, A.L., Randall, R.J., 1951. Protein measurement with the Folin phenol reagent. *J. Biol. Chem.* 193, 265–275.

Monroig, Ó., Li, Y., Tocher, D.R., 2011a. Delta-8 desaturation activity varies among fatty acyl desaturases of teleost fish: high activity in delta-6 desaturases of marine species. *Comp. Biochem. Physiol. Part B Biochem. Mol. Biol.* 159, 206–213.

Monroig, Ó., Webb, K., Ibarra-Castro, L., Holt, G.J., Tocher, D.R., 2011b. Biosynthesis of long-chain polyunsaturated fatty acids in marine fish: characterization of an Elov14-like elongase from cobia *Rachycentron canadum* and activation of the pathway during early life stages. *Aquaculture* 312, 145–153.

Monroig, Ó., Wang, S., Zhang, L., You, C., Tocher, D.R., Li, Y., 2012. Elongation of long-chain fatty acids in rabbitfish *Siganus canaliculatus*: cloning, functional characterisation and tissue distribution of Elov15- and Elov14-like elongases. *Aquaculture* 350–353, 63–70.

Monroig, Ó., Lopes-Marques, M., Navarro, J.C., Hontoria, F., Ruivo, R., Santos, M.M., Venkatesh, B., Tocher, D.R., Castro, L.F.C., 2016. Evolutionary functional elaboration of the Elov12/5 gene family in chordates. *Sci. Rep.* 6, 1–10.

- Monroig, Ó., Tocher, D.R., Castro, L.F.C., 2018. Polyunsaturated fatty acid biosynthesis and metabolism in fish. In: Burdge, G. (Ed.), *Polyunsaturated Fatty Acid Metabolism*. AOCS Press, London, pp. 31–60.
- Morais, S., Castanheira, F., Martínez-Rubio, L., Conceição, L.E.C., Tocher, D.R., 2012. Long chain polyunsaturated fatty acid synthesis in a marine vertebrate: ontogenetic and nutritional regulation of a fatty acyl desaturase with  $\Delta 4$  activity. *Biochim. Biophys. Acta Mol. Cell Biol. Lipids* 1821, 660–671.
- Morais, S., Mourente, G., Martínez, A., Gras, N., Tocher, D.R., 2015. Docosahexaenoic acid biosynthesis via fatty acyl elongase and  $\Delta 4$ -desaturase and its modulation by dietary lipid level and fatty acid composition in a marine vertebrate. *Biochim. Biophys. Acta Mol. Cell Biol. Lipids* 1851, 588–597.
- Mourente, G., Tocher, D.R., 1993a. Incorporation and metabolism of  $^{14}\text{C}$ -labelled polyunsaturated fatty acids in juvenile gilthead sea bream *Sparus aurata* L. in vivo. *Fish Physiol. Biochem.* 10, 443–453.
- Mourente, G., Tocher, D.R., 1993b. Incorporation and metabolism of  $^{14}\text{C}$ -labelled polyunsaturated fatty acids in wild-caught juveniles of golden grey mullet, *Liza aurata*, in vivo. *Fish Physiol. Biochem.* 12, 119–130.
- Mourente, G., Tocher, D.R., 1994. In vivo metabolism of [ $^{14}\text{C}$ ] linolenic acid (18: 3 (n–3)) and [ $^{14}\text{C}$ ] eicosapentaenoic acid (20: 5 (n–3)) in a marine fish: time-course of the desaturation/elongation pathway. *Biochim. Biophys. Acta Lipids Lipid Metab.* 1212, 109–118.
- Mourente, G., Dick, J.R., Bell, J.G., Tocher, D.R., 2005. Effect of partial substitution of dietary fish oil by vegetable oils on desaturation and  $\beta$ -oxidation of [ $^{14}\text{C}$ ] 18: 3n-3 (LNA) and [ $^{14}\text{C}$ ] 20: 5n-3 (EPA) in hepatocytes and enterocytes of European sea bass (*Dicentrarchus labrax* L.). *Aquaculture* 248, 173–186.
- Oboh, A., Kabeya, N., Carmona-Antoñanzas, G., Castro, L.F.C., Dick, J.R., Tocher, D.R., Monroig, Ó., 2017. Two alternative pathways for docosahexaenoic acid (DHA, 22:6n-3) biosynthesis are widespread among teleost fish. *Sci. Rep.* 7, 3889.
- Pérez, J.A., Rodríguez, C., Henderson, R.J., 1999. The uptake and esterification of radiolabelled fatty acids by enterocytes isolated from rainbow trout (*Oncorhynchus mykiss*). *Fish Physiol. Biochem.* 20, 125–134.
- Pérez, J.A., Rodríguez, C., Bolaños, A., Cejas, J.R., Lorenzo, A., 2014. Beef tallow as an alternative to fish oil in diets for gilthead sea bream (*Sparus aurata*) juveniles: effects on fish performance, tissue fatty acid composition, health and flesh nutritional value. *Eur. J. Lipid Sci. Technol.* 116, 571–583.
- Rodríguez, C., Pérez, J.A., Henderson, R.J., 2002. The esterification and modification of n-3 and n-6 polyunsaturated fatty acids by hepatocytes and liver microsomes of turbot (*Scophthalmus maximus*). *Comp. Biochem. Physiol. B Biochem. Mol. Biol.* 132, 559–570.
- Ruyter, B., Sissener, N.H., Østbye, T.K., Simon, C.J., Krasnov, A., Bou, M., Sanden, M., Nichols, P.D., Lutfi, E., Berge, G.M., 2019. n-3 Canola oil effectively replaces fish oil as a new safe dietary source of DHA in feed for juvenile Atlantic salmon. *Br. J. Nutr.* 122, 1329–1345.
- Sprague, M., Dick, J.R., Tocher, D.R., 2016. Impact of sustainable feeds on omega-3 long-chain fatty acid levels in farmed Atlantic salmon, 2006–2015. *Sci. Rep.* 6, 21892.
- Sprecher, H., 2000. Metabolism of highly unsaturated n-3 and n-6 fatty acids. *Biochim. Biophys. Acta Mol. Cell Biol. Lipids* 1486, 219–231.
- Tocher, D.R., 2015. Omega-3 long-chain polyunsaturated fatty acids and aquaculture in perspective. *Aquaculture* 449, 94–107.
- Tocher, D.R., Ghioni, C., 1999. Fatty acid metabolism in marine fish: low activity of fatty acyl  $\Delta 5$  desaturation in gilthead sea bream (*Sparus aurata*) cells. *Lipids* 34, 433–440.
- Tocher, D.R., Betancor, M.B., Sprague, M., Olsen, R.E., Napier, J.A., 2019. Omega-3 long-chain polyunsaturated fatty acids, EPA and DHA: bridging the gap between supply and demand. *Nutrients* 11, 89.
- Trushenski, J.T., Rombenso, A.N., 2019. Trophic levels predict the nutritional essentiality of polyunsaturated fatty acids in fish-introduction to a special section and a brief synthesis. *N. Am. J. Aquac.* <https://doi.org/10.1002/naaq.10137>.
- Vandesompele, J., De Preter, K., Pattyn, F., Poppe, B., Van Roy, N., De Paepe, A., Speleman, F., 2002. Accurate normalization of real-time quantitative RT-PCR data by geometric averaging of multiple internal control genes. *Genome Biol.* 3 (7) research 0034.
- Wilson, R., Sargent, J.R., 1992. High-resolution separation of polyunsaturated fatty acids by argentation thin-layer chromatography. *J. Chromatogr. A* 623, 403–407.
- Zar, J.H., 1999. *Biostatistical Analysis*, 4th ed. Prentice-Hall Inc., Upper Saddle River.
- Zárate, R., el Jaber-Vazdekis, N., Tejera, N., Pérez, J.A., Rodríguez, C., 2017. Significance of long chain polyunsaturated fatty acids in human health. *Clin. Transl. Med.* 6, 25.
- Zheng, X., Ding, Z., Xu, Y., Monroig, Ó., Morais, S., Tocher, D.R., 2009a. Physiological roles of fatty acyl desaturases and elongases in marine fish: characterisation of cDNAs of fatty acyl  $\Delta 6$  desaturase and elov15 elongase of cobia (*Rachycentron canadum*). *Aquaculture* 290, 122–131.
- Zheng, X., Leaver, M.J., Tocher, D.R., 2009b. Long-chain polyunsaturated fatty acid synthesis in fish: comparative analysis of Atlantic salmon (*Salmo salar* L.) and Atlantic cod (*Gadus morhua* L.)  $\Delta 6$  fatty acyl desaturase gene promoters. *Comp. Biochem. Physiol. B Biochem. Mol. Biol.* 154, 255–263.